LAPPEENRANTA UNIVERSITY OF TECHNOLOGY
LUT School of Energy Systems
LUT Mechanical Engineering

Muhammad Awais

ENHANCING THE 3-DIMENSIONAL FORMING OF PAPERBOARD WITH MODELLING AND SIMULATION

Examiners: Professor Kaj Backfolk
Associate Professor Joonas Sorvari

ABSTRACT

Lappeenranta University of Technology
LUT School of Energy Systems
LUT Mechanical Engineering

Muhammad Awais

Enhancing the 3-dimensional forming of paperboard tray with modelling and simulation

Master's thesis

2016

69 pages, 67 figures, 10 table and 1 appendice

Examiners: Professor Kaj Backfolk
Associate Professor Joonas Sorvari

Keywords: Paperboard, material properties, single ply paperboard, multiply paperboard, creases.

This thesis work was based on the enhancing of 3-dimensional forming of paperboard tray package by adopting line creasing pattern and analysis of the results with the help of mathematical modelling and simulation. The aim of the project is to improve convertibility of paperboard blank in tray forming by replacing linear creased pattern around the corner areas. The paperboard with and without creases was modelled and their relevant stresses, total strain and plastic strain was compared. Two different paperboards named single ply and multiply paperboard were simulated. The comparison revealed that the creases improved the performance and convertibility of paperboard by reducing stiffness. The reaction force from paperboard blank on female die was calculated and curve follows the experimental behavior measured with the help of four sensors. The project was sponsored by Stora Enso and lasted for six months.

ACKNOWLEDGEMENTS

This work was carried out as a part of the RR Coat-project under the collaboration of Stora Enso Oyj and Lappeenranta University of technology. I thank to Jari Räsänen, Risto Vapola, Mari Hiltunen and Henry Lindell who provided me opportunity to take part in the research and development of Stora Enso.

I thank to Joonas Sorvari, Associate Professor for his supervision and assistance with ABAQUS modules, Python scripts and comments that greatly improved my research focus. Under his supervision, my approach was target oriented and I achieved my milestones within allocated time.

I would also like to show my gratitude to my project manager, Panu Tanninen (D.Sc.) for sharing his expert opinions in comparison of simulated results and experimental data. I am also immensely grateful to Sami Matthews to guide me with design module.

Muhammad Awais

Lappeenranta 30.9.2015

TABLE OF CONTENTS

LIST OF SYMBOLS AND ABBREVIATIONS

ξ	Anisotropy
E_{ij}	Elastic modulus (N/mm^2)
$\varepsilon_{elastic}$	Elastic strain
σ_{ij}^{0}	Initial yield stress
$\varepsilon_{plastic}$	Plastic strain
ν_{ij}	Poisson ratio
G_{ij}	Shear modulus (N/mm^2)
γ_{ij}	Shear tensor (N/mm^2)
σ_{11}	Stress component along x direction with respect to x
σ_{21}	Stress component along y direction with respect to x
σ_{31}	Stress component along z direction with respect to x
σ_{ij}	Stress tensor (N/mm^2)
τ_{ij}	Stress tensor (rotational) (N/mm^2)
F_j	Summation of forces from x, y and z direction
ε_{total}	Total strain
D	Vector of unknowns
F	Constant in Hill's yielding expression
G	Constant in Hill's yielding expression
H	Hardening modulus
K	Matrix of unknown constants
M	Constant in Hill's yielding expression
R	Vector of known loads
AC2D4	4-node linear 2-D acoustic quadrilateral, reduced integration, hourglass control
CAD	Computer aided design

CAX4R	4-node bilinear axisymmetric quadrilateral, reduced integration, hourglass control
CD	Cross direction
CPE4	4-node bilinear plane strain quadrilateral, reduced integration, hourglass control
FEM	Finite element method
FM	Female mold
MD	Machine direction
MM	Male mold
PDE	Partial differential equations
PET	Polyethylene terephthalate
RP	Reference point
RTF	Rim tool force
S4R	4-node doubly curved shell, reduced integration, hourglass control, finite membrane strains

1 INTRODUCTION

Paper and paperboard plays a vital role in different types of packaging. Paper-based products are worthy of importance in daily consumption over plastic based packaging materials because of renewability, recyclability, biodegradability and sustainability. Paperboard chemistry also has a key role in sustainability and performance of modern packages in variant environmental conditions. The formability of paperboard can be improved by chemical and mechanical modification of fibers.

Three dimensional forming technique is used to produce aesthetic and advanced shapes from paperboard but still performance of paper and paperboard based packages depend upon understanding of mechanical parameters of forming. Plastic based packages, on the other hand have wide variety of forming processes. (Vishtal et al. 2013, p. 677.) The major limitation in 3-dimensional forming of paperboard is its poor formability or rather its capability to withstand large deformation without damage.

Three dimensional formability is an intricate mechanical property of paperboard that determines the prime performance of multiplex material. Formability is a subject of conventional deep drawing process in paperboard products and used to form tray packages, cups and various consumer packages (see Figure 1). The formability of paper or paperboard especially in deep drawing process is highly depend on mechanical properties: compression, elongation, strain, strength, paper to metal friction (Vishtal et al. 2013, p. 677). The role of each property, influence the formability process in respect to the depth of the proposed design. In 3-dimensional forming, the paperboard is compelled to slide along edges or corner of cavity with large force, while the paperboard is tightened in between dies. The friction force resists transverse compressive deformation and causes wrinkles and other defects.

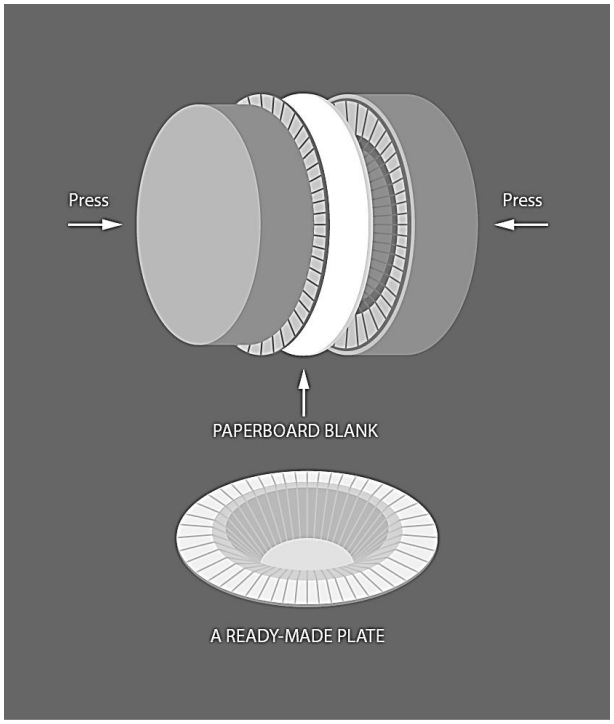

Figure 1. Deep drawing of paperboard tray package (Iggesund 2016a).

1.1 FEM and forming

Packages can be made more flexible and customized to benefit the producer, customers and also environment. Research has already been done to improve the performance, convertibility and sustainability of the product.

Similar to plastic and metal, deep drawing process is vitally used for the forming of paper or paperboard tray package. Corners are the critical zones because of large force which sometime causes smear and fracture of round surface. Material direction of paperboard impacts the overall properties of the end product. Forming of paperboard is a complex mechanism in which there are many deformation and damage mechanisms that are still unknown. (Huang & Nygårds 2012, p. 221.) Some of the complex factors such as anisotropy, thickness direction gradients, and moisture and temperature dependency are worthy to study.

Paperboard has anisotropic properties, during deformation it shows wrinkles and cracks compare to metal forming. Structurally, it is composed of three to five layers or plies. During the formation of paperboard, the paper web flows in the direction of machine refer as machine direction (MD) and the direction perpendicular to MD is called cross direction

(CD). Moreover, out of plane properties also influence the dimension stability of paperboard called z-direction, or out of plane. (Huang et al. 2012, p. 221.)

Currently, two major process are used to form a paperboard surface. Suspension of fibers is sprayed onto a die of the desired shape. Complex and intricate shapes can be achieved by this method. Egg box is one example of this method. Another technique is application of load on paperboard sheet into the female die with the help of male die under support of blank holder (see Figure 2). Friction plays an important role in order to attain desired shape. Alternatively, load can be applied by a membrane using pressurized air or liquid over concave side of die or package. Deep drawing has advantage over spraying fiber method because it maintain high stiffness and strength of package. (Huang et al. 2012, p. 221.)

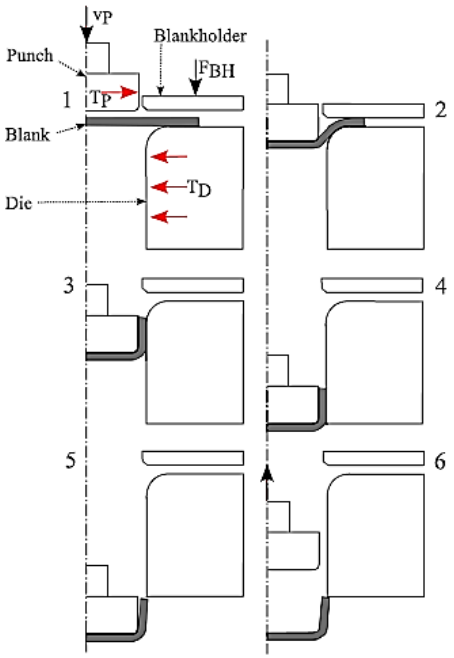

Figure 2. Paperboard tray formed by deep drawing method (Wallmeier et al. 2015, p. 202).

The deep drawing process for forming of paperboard has been investigated for over a century. The research that supports this mechanism was taken into consideration in the 1930's by Schere, who scrutinized theoretical fundamental of tool design and parameters related to the forming process. Heinz continued this research and investigated the attributes of the punch force curve. However, deep drawing is still consider as a technical and highly flexible process to deal with three dimensional forming of the paperboard. In comparison to

embossing, higher forming degrees can be achieved by the deep drawing process. (Wallmeier et al. 2015, p. 202.)

Innovative packaging design and concepts are the preliminary reason to conduct scientific research in the field of paperboard. Hence use of biodegradable paper based material improve the network of resources and border use. The main stage include the primary packaging that has high functional and visual demands. (Wallmeier et al. 2015, p. 202.)

Paperboard was not worthy of consideration until potential research revealed the importance of 3 dimensional forming processes. One of an important parameter is the blank holder exerting forces on paperboard during forming into complex curve geometry to avoid wrinkling and discoloration. Mold, blank holder forces and metal friction, are the main factors to consider in order to improve complex geometries. Geometric parameters show close dependencies on each other and require experimental work. The enhancement in intricate geometries, or shape diversity and visual quality respective of its physical mechanisms are still not well explained, and need further development. During the deep drawing process, change in one parameter changes multiple effect on mechanical and material properties. The analysis of material properties in deep drawing process of paperboard forming is a difficult issue. (Wallmeier et al. 2015, p. 203.)

The hydroforming process is closely related to mechanism of deep drawing. It deals with paperboard blank deformation into a cavity with the help of membrane and material start expansion without compression. Whereas in deep drawing, paperboard blank is forced by the male tool to stretch into the female cavity and compressional forces are exerted on paperboard surfaces. (Wallmeier et al. 2015, p. 203.)

The deformation of paper or paperboard under load is a three dimensional problem. Deformation in 3D means that it is not only in the direction of loading but also across the plane (perpendicular to loading direction). Paper and paperboard usually show the increase in thickness when specimen is subjected to compressive strain directed in plane. Poisson effect is defined in term of Poisson ratio (negative of ratio of strain in cross loading and loading direction). Out of plane Poisson ratio plays a significant role in 3D constitutive model that can deal with related problems where thickness variation is of worthy to study.

Thickness properties also implies great effect in converting process. Thickness is usually reduced to improve surface smoothness. Paper material both have positive and negative Poisson ratio value. Stiffness values along MD direction is about 1 to 5 times greater than CD, 100 time large compared to ZD. Paper is consider as orthotropic material. (Stenberg & Fellers 2002, p. 387.)

1.2 Objective

This project deals with 3-dimensioanl forming of paperboard with the help of mathematical modelling and simulation. The research is focused to examine deformation and forming of paperboard with different crease pattern and comparison of results. The main aim is to enhance the convertibility of paperboard with the help of creases. Linear crease pattern was of high importance and investigated in the present research. In order to analyze the mechanical behavior of paperboard tray package around corners, modelling is done using finite element software Abaqus.

Firstly, paperboard without creases referred as plane paperboard, was modeled and simulated under the influence of loading by male die against female die and the critical loading zones were analyzed. Secondly, linear crease pattern was modelled and hinge joint in Abaqus was used to model the behavior of creases. Corner areas were the center of attention in the linear crease paperboard. Finally, results obtained from plane and creased paperboard were evaluated.

The total strain, plastic strain and von Mises stresses were calculated and compared. Efficiency and accuracy of measurement procedure were valued.

1.3 Paperboard

Paper and paperboard is most commonly used materials in industries because of recyclability, degradability, environment friendly. First paperboard was made using cellulose fibers from flax, cotton and vegetable sources around 105 A.D. Nowadays, still paperboard manufacturing process begins with separating cellulose fibers originated from renewable raw material. The fundamental structure of sheet or web is comprise of an interlaced network of fibers. A dilute suspension of fibers begin this process and water contents are removed by evaporation and drainage. The primarily source of fibers is wood.

These fiber are separated by chemical or mechanical methods from naturally occurring source of birch, pine or spruce. (Amigo 2012, p. 1.)

Two basic types of fibers are used in manufacturing of paperboard, mechanical and chemical processed fibers of wood. Different treatments induces variant properties on pulps or paperboard that overall effects the paperboard properties (See Figure 3). Specific combination of fiber orientation and whiteness are consider to fulfill appearance and performance demand. (Iggesund 2016b.)

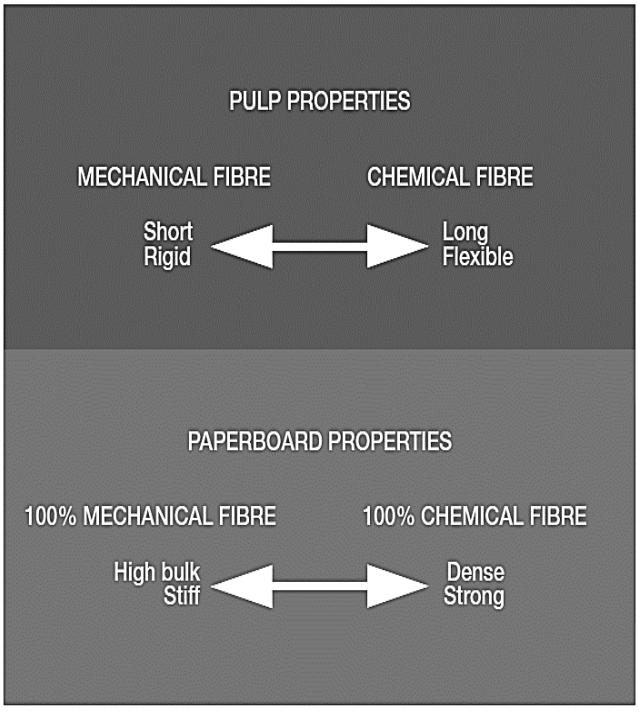

Figure 3. Pulp Properties and influence on paperboard properties (Iggesund 2016b).

Paperboard comprise of thick, single or multiply fiber based material. The middle ply of paperboard is bulky compared to upper and lower ply. This formation relates to I-beam structure where higher stiffness can be achieved with few fibers. The bending stiffness is an important mechanical property for paperboard package. Outer ply of paperboard mainly contribute to bending stiffness with higher density. Middle ply attributed less to bending stiffness because of its own low bending stiffness and function of separating upper and lower ply. Combination of lower density of middle ply and higher density of surface plies made overall higher bending stiffness of paperboard. In manufacturing, each ply is made separately and stack with each other to attain required properties.

1.3.1 Press forming mechanism

The mechanism of press forming follows the precutting and creasing patterns on paperboard. Paperboard blank of specific dimensions is then placed in between male (MM) and female mould (FM). Male die provide force to press paperboard into the female mould cavity. In order to avoid wrinkles and control the creases around corners, constant blank holding force (RTF-orange) presses blank against female tool (see Figure 4). Male tool remain at the bottom end of stock for set time called as dwell time. Furthermore, adjacently blank holder presses to flatten the paperboard tray edges. (Tanninen 2015, p. 19.)

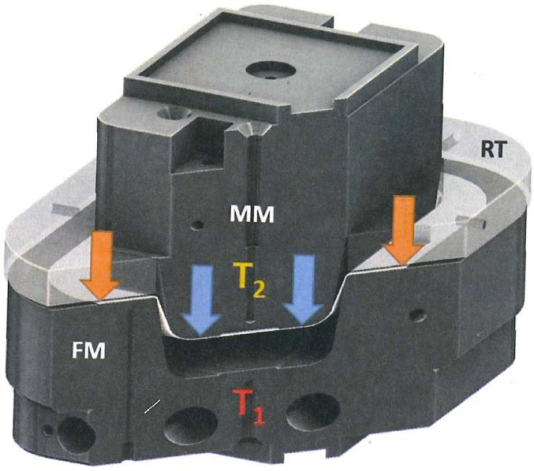

Figure 4. Press forming tool (MM-Male die pressing force, RT- Blank holder force, T_1-Female tool temperature and T_2-Male tool temperature) (Tanninen 2015, p. 19).

2 MATERIAL MODEL AND METHODS

The mechanical behavior of material govern physical laws that depicts the intrinsic properties of continuous material or individual material. These laws interpret mass conservation, equilibrium of momentum and forces and conservation of total energy. Three dimensional loading problems include strong influence of stresses, strain and displacement (internal or external). In some cases, magnitude and distribution of stresses are important while on the other hand, stiffness and deformation are area of interest. Excessive distortion of a solid body under influence of external loading, justify three governing equations: (1) equilibrium; (2) kinematics; and (3) material constitution. Material constitutive equation is the only one that depends on material type. It represent material properties and mechanical behavior. (Findley, Lai & Onaran 1976, p. 40.)

Equation governs behind the 3-D forming of paperboard follows static equilibrium in which resultant of all forces is zero. The equilibrium along x direction can sum up as

$$\begin{aligned}&(\sigma_{11}+\frac{\partial\sigma_{11}}{\partial x_1}dx_1)dx_2dx_3-\sigma_{11}dx_2dx_3+(\sigma_{21}+\frac{\partial\sigma_{21}}{\partial x_2}dx_2)dx_1dx_3-\sigma_{21}dx_1dx_3\\&+(\sigma_{31}+\frac{\partial\sigma_{31}}{\partial x_3}dx_3)dx_2dx_1-\sigma_{31}dx_2dx_1+F_1dx_1dx_2dx_3=0\end{aligned} \tag{1}$$

Where σ_{11} represents stress component along x-direction, σ_{21} is the stress along x direction with respect to y component of stress and σ_{31} is stress along x direction with respect to z component of stress. (Findley et al. 1976, p. 42.)

Similarly, equation along y and z direction can be obtained. By dividing equation 1. With $dx_1dx_2dx_3$, it will give equation on each direction of coordinate axes.

$$\begin{aligned}
&\frac{\partial \sigma_{11}}{\partial x_1} + \frac{\partial \sigma_{21}}{\partial x_2} + \frac{\partial \sigma_{31}}{\partial x_3} + F_1 = 0, \\
&\frac{\partial \sigma_{12}}{\partial x_1} + \frac{\partial \sigma_{22}}{\partial x_2} + \frac{\partial \sigma_{32}}{\partial x_3} + F_2 = 0, \\
&\frac{\partial \sigma_{13}}{\partial x_1} + \frac{\partial \sigma_{23}}{\partial x_2} + \frac{\partial \sigma_{33}}{\partial x_3} + F_3 = 0.
\end{aligned} \tag{2}$$

Equation 2 can be express in tensor form as

$$\frac{\partial \sigma_{ij}}{\partial x_i} + F_j = 0 \tag{3}$$

, where F_j is the summation of forces from x, y and z direction. (Findley et al. 1976, p. 42.)

2.1 Anisotropy of paperboard

Paperboard is an anisotropic and heterogeneous material. It is difficult and challenging to model paperboard. Fibers are scattered at wide range of angles in paperboard. MD acted as reference and fibers that are at an angle with MD and direction of maximum deformation represented by an angle θ (see Figure 5). Anisotropy is expressed by a/b=ξ where a and b calculated by distribution. Within the structure of fibers, anisotropy is described by length of fiber segment (see Figure 6). Longer the length, stronger will be the anisotropy. (Leppänen et al., 2005, p. 842.)

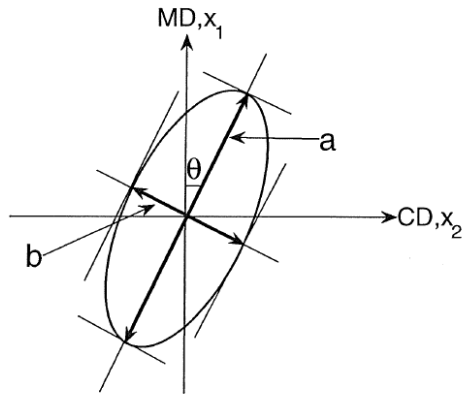

Figure 5. θ is an angle between MD and maximum oriented fibers (Leppänen et al., 2005, p 843).

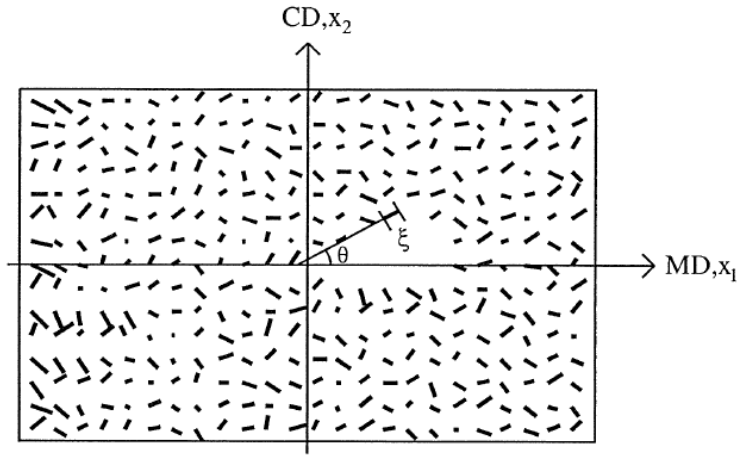

Figure 6. Single layer of paperboard fibers where length describe anisotropy (Leppänen et al. 2005, p. 843).

Paperboard material follows Hooks law and behave as plastic material after yield point (See Figure 7). For orthotropic materials, Hill's criteria can be used to describe yielding. Fibers within elastic limit elongate elastically whereas after elastic limit, interlocking of fibers cause plastic deformation.

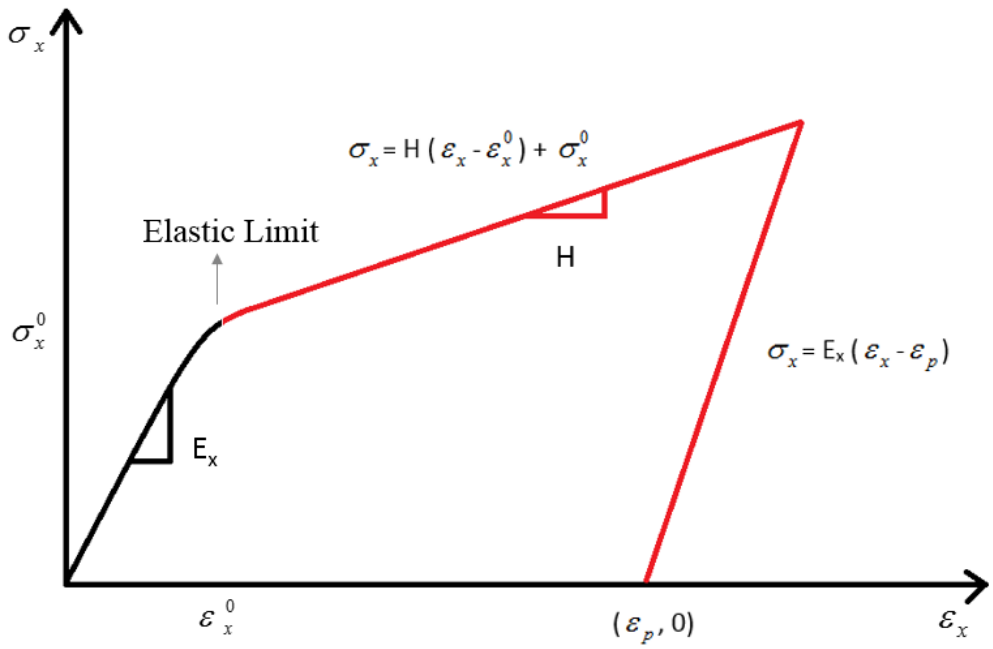

Figure 7. Graphical illustration of behavior of paperboard material.

Where σ_x and ε_x represent stress and strain component along x direction. Furthermore, yield stress and strain components are presented by σ_x^o and ε_x^o. The residual plastic strain is represented by ε_p. E_x and H are Young's modulus and hardening modulus.

2.2 Elastic material model

The elastic material model of paperboard can be expressed by continuum material model as well as interface material model. Continuum material model was used during the analysis.

2.2.1 Continuum model

In this thesis work, two different type of paperboards were modelled; named single ply and multiply paperboard. Anisotropy of paperboard is a complex attribute in 3D forming which can cause numerical problem in convergence of solution. Elastic model for an orthotropic material can be described as

$$\begin{bmatrix} \varepsilon_{xx} \\ \varepsilon_{yy} \\ \varepsilon_{zz} \\ \gamma_{xy} \\ \gamma_{xz} \\ \gamma_{yz} \end{bmatrix} = \begin{bmatrix} \frac{1}{E_x} & -\frac{v_{yx}}{E_y} & -\frac{v_{zx}}{E_z} & 0 & 0 & 0 \\ -\frac{v_{xy}}{E_x} & \frac{1}{E_y} & -\frac{v_{zy}}{E_z} & 0 & 0 & 0 \\ -\frac{v_{xz}}{E_x} & -\frac{v_{yz}}{E_y} & \frac{1}{E_z} & 0 & 0 & 0 \\ 0 & 0 & 0 & \frac{1}{G_{xy}} & 0 & 0 \\ 0 & 0 & 0 & 0 & \frac{1}{G_{xz}} & 0 \\ 0 & 0 & 0 & 0 & 0 & \frac{1}{G_{yz}} \end{bmatrix} \begin{bmatrix} \sigma_{xx} \\ \sigma_{yy} \\ \sigma_{zz} \\ \tau_{xy} \\ \tau_{xz} \\ \tau_{yz} \end{bmatrix} \tag{4}$$

In equation 4 the σ_{xx}, σ_{yy}, σ_{zz}, τ_{xy}, τ_{xz} and τ_{yz} expressed as components of stress tensor (N/mm^2), $E_x, E_y, E_z, G_{xy}, G_{xz}$ and G_{yz} are elastic and shear modulus expressed in N/mm^2 and $\varepsilon_{xx}, \varepsilon_{yy}, \varepsilon_{zz}, \gamma_{xy}, \gamma_{xz}$, and γ_{yz} are components of strain tensor. (Huang 2013, p. 07.)

Proper definition of material model include evaluation of constants in Equation 1. E_{xx}, E_{yy}, E_{zz} represents Young's moduli in different principal orientation (MD, CD and z

direction). G_{xy}, G_{xz} and G_{yz} variables demonstrate shear moduli and $\nu_{xy}, \nu_{yx}, \nu_{xz}, \nu_{zx}, \nu_{yz}$, ν_{zy} are Poisson's ratio. There are six variables of Poisson ratio to determine due to anisotropy but three of them are independent because of matrix compliance symmetry. Therefore, nine constants determine the material behavior for one layer. Tensile properties of layers can be calculated by considering paperboard as homogeneous material. (Amigo 2012, p. 7.)

E_{xx} along machine direction and E_{yy} along cross direction and can be calculated by tensile test. In tensile test of paperboard, sample strip of paperboard of standard size is fixed within jaws and force and displacement is measured relatively. These experiment can find Young's modulus in both MD and CD. The value of Young's Modulus along Z direction E_{zz} can be determine by respective values of tensile test. (Amigo 2012, p. 8.)

$$E_{zz} = \frac{E_{xx}}{200} \tag{5}$$

Similarly, shear modulus G_{xy}, G_{xz}, and G_{yz} can be determined with the help of following equations.

$$G_{xy} = 0.39 * \sqrt{E_{xx} * E_{yy}} \tag{6}$$

$$G_{xz} = \frac{E_{xx}}{55} \tag{7}$$

$$G_{xz} = \frac{E_{yy}}{35} \tag{8}$$

Poisson ratios that are independent are calculated and respective values are derived from measured ones. Equations show the relationship of Poisson ratios. (Amigo 2012, p. 8.)

$$\frac{\nu_{xy}}{E_{xx}} = \frac{\nu_{yx}}{E_{yy}} \tag{9}$$

$$\frac{\nu_{xz}}{E_{xx}} = \frac{\nu_{zx}}{E_{yy}} \tag{10}$$

$$\frac{\nu_{yz}}{E_{yy}} = \frac{\nu_{zy}}{E_{zz}} \tag{11}$$

2.3 Plastic material model

After elastic limit, yielding or interlocking of fibers cause plastic behavior. Moreover, stress components σ_{ij} are used to describe yielding of paperboard. The Hill's criteria can be expressed as

$$f(\sigma)=\sqrt{F(\sigma_{yy}-\sigma_{zz})^2+G(\sigma_{zz}-\sigma_{xx})^2+M(\sigma_{xx}-\sigma_{yy})^2+\frac{(\sigma_{xx}^0)^2}{(\sigma_{yz}^0)^2}\sigma_{yz}^2+\frac{(\sigma_{xx}^0)^2}{(\sigma_{xz}^0)^2}\sigma_{xz}^2+\frac{(\sigma_{xx}^0)^2}{(\sigma_{xy}^0)^2}\sigma_{xy}^2} \quad (12)$$

Where σ_{ij}^0 represents initial yield stresses in different orientations, F, G and M can be represent as

$$F=\frac{(\sigma_{xx}^0)^2}{2}(\frac{1}{(\sigma_{yy}^0)^2}+\frac{1}{(\sigma_{zz}^0)^2}-\frac{1}{(\sigma_{xx}^0)^2} \quad (13)$$

$$G=\frac{(\sigma_{xx}^0)^2}{2}(\frac{1}{(\sigma_{zz}^0)^2}+\frac{1}{(\sigma_{xx}^0)^2}-\frac{1}{(\sigma_{yy}^0)^2} \quad (14)$$

$$M=\frac{(\sigma_{xx}^0)^2}{2}(\frac{1}{(\sigma_{xx}^0)^2}+\frac{1}{(\sigma_{yy}^0)^2}-\frac{1}{(\sigma_{zz}^0)^2} \quad (15)$$

In paperboard, hardening behavior follows hardening modulus H. Value of H can be calculated by tensile test of harden material in machine direction (MD). (Huang 2011, p. 212.)

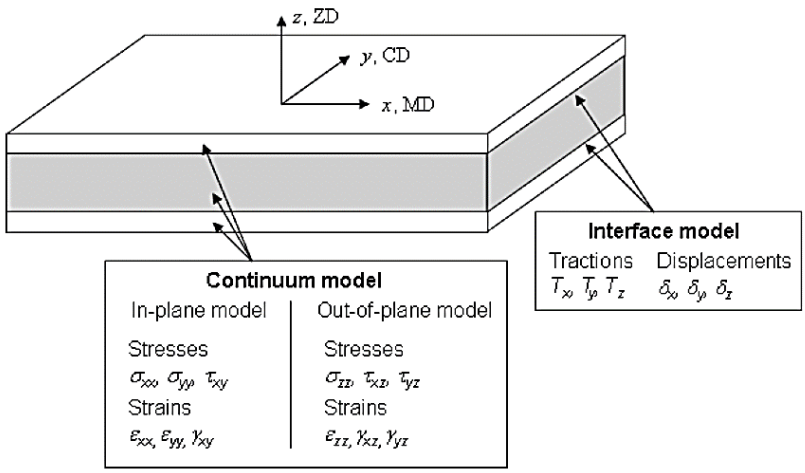

Figure 8. Numerical models of paperboard (Huang 2011, p. 19).

In modelling, only continuum material model was followed ignoring interface model.

2.4 Material properties

Characterization of material reveals the general properties to explain mechanical behavior and factor influencing the mechanical properties. In order to attain approximate simulated results, measurement of material properties should be accurate and precise. Influence of some properties are very less during paperboard forming and can be empirically calculated using literature data.

Paperboard material behave as linearly elastic orthotropic material, hence material shows deformation proportionally to applied stress. After a certain proportional elastic limit, paperboard behaves plastically due to interlocking of fibers. In this thesis, paperboard was consider as elastoplastic that follows Hook's law and Hill's yielding criteria. Fracture or failure of paperboard is not considered. The elastoplastic material model used in this thesis, was adopted from literature presented by Huang (2012). The material properties are given in Table 1 and 2.

Table 1. Material model constants (Mod. Huang at al. 2012, p. 225).

Constants	Top ply	Middle ply	Bottom ply
E_{xx} (MPa)	5920	3202	8760
E_{yy} (MPa)	2670	1233	3030
E_{zz} (MPa)	228	160	130
G_{xy} (MPa)	1431	638	1617
G_{xz} (MPa)	60	30	68
G_{yz} (MPa)	60	30	68
v_{xy}	0.45	0.47	0.51
v_{xz}	0	0	0
v_{yz}	0	0	0

Table 1 continues. Material model constants (Mod. Huang at al. 2012, p. 225).

H (MPa)	2289	802	4288
σ_{xx}^{0} (MPa)	40	22	66
σ_{yy}^{0} (MPa)	14.2	10.1	24
σ_{zz}^{0} (MPa)	14.2	10.1	24
σ_{xy}^{0} (MPa)	28	13.2	33
σ_{xz}^{0} (MPa)	4.8	0.66	3.96
σ_{yz}^{0} (MPa)	3.48	0.28	2.97
R_{11}	1	1	1
R_{22}	0.3550	0.4590	0.3636
R_{33}	0.3550	0.4590	0.3636
R_{12}	1.2124	1.0392	0.8660
R_{13}	0.2078	0.0519	0.1039
R_{23}	0.1506	0.0220	0.0779

Table 2. Yield stress and plastic strain of paperboard.

Top ply		Middle ply		Bottom ply	
Yield stress	Plastic strain	Yield stress	Plastic strain	Yield stress	Plastic strain
40 MPa	0	22 MPa	0	60 MPa	0
268.9 MPa	0.1	102.2 MPa	0.1	494.8 MPa	0.1
1184.5 MPa	0.5	423 MPa	0.5	2210 MPa	0.5

2.5 Finite element method

The FE method can be defined as, according to Cook (1995, p. 1) “A piecewise polynomial interpolation. A field quantity such as displacement is interpolated from values of the field quantity at nodes. By connecting elements together, the field quantity becomes interpolated over the entire structure in piecewise fashion by as many polynomial expressions as there are elements. The minimization process generate a set of simultaneous algebraic equations

of the field quantity at nodes". Furthermore, According to Amigo (2012, p. 3) "The FEM is a numerical technique for finding approximate solutions of partial differential equations (PDE) as well as integral equations".

FEM involves

- The structure is divided into finite elements
- Then reconnect the elements at "nodes": considering nodes as pins to hold the elements together
- The whole process results in a set of simultaneous algebraic equations.

For linear problems the set of equations can be expressed by matrix symbolism as

$$KD = R \tag{16}$$

In equation 16, the D is a vector of unknowns, R represents vector of known loads and K is matrix of unknown constants. (Cook 1995, p. 01.)

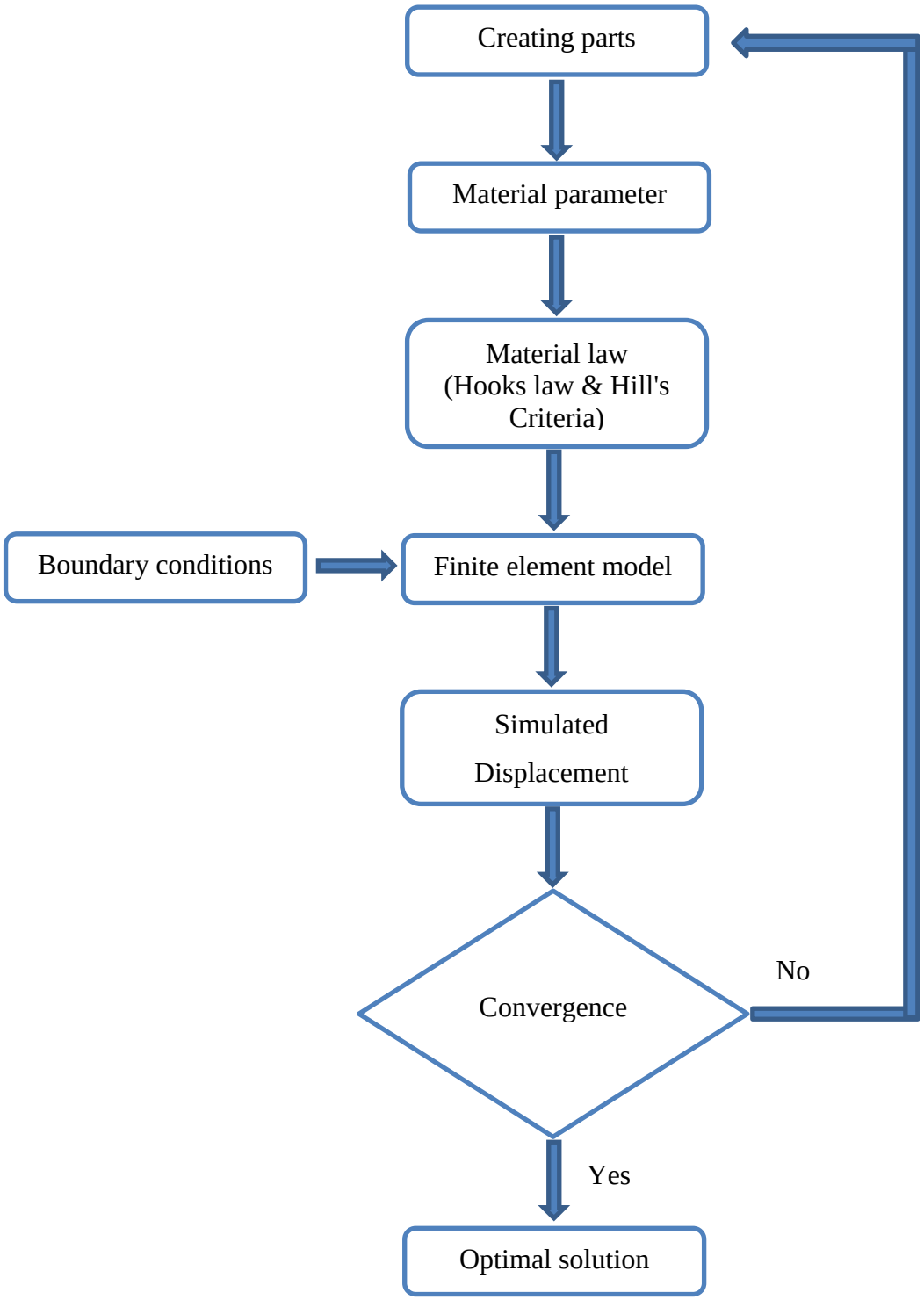

Figure 9. Flowchart of FEA.

2.6 Abaqus

Abaqus is finite element analysis software that provide solution of real world engineering problems by using mathematical techniques. Flexibility in design and solution module, made Abaqus one of the leading software to analyze intractable engineering problems.

Abaqus was initially designed to deal with nonlinear problems but extension provided the complete solution regarding material models such as elastic, plastic of material. It has an extensive use in automobile, aerospace and petroleum industries. Due to its flexibility and adaptability, it is common in research institutes and academics. It also has multiple modules to solve acoustic structure, piezoelectric and structural problems. Abaqus solve the problem in three main stages (see Figure 10).

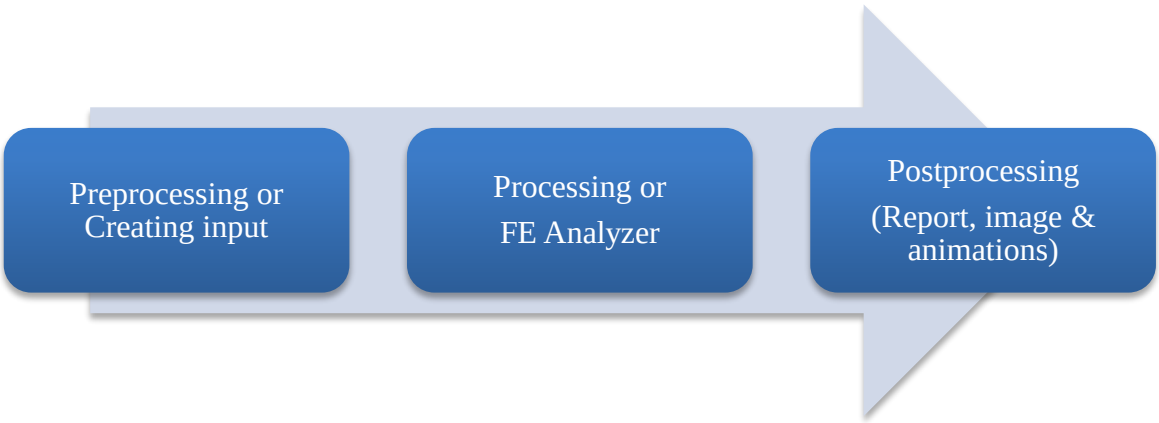

Figure 10. Stages of finite element analysis.

Abaqus provide user freedom of preprocessing, post processing and investigation of problem at different time steps. Preprocessing stage can be done by using other computer aided design (CAD) software such as Solid works, Pro E, Creo. Files of different format can be import or export into or from Abaqus. Current research was done by using Abaqus 6.14, no other CAD software was not used. Individual parts were modelled using design module in Abaqus. Deep drawing process was implemented using Abaqus Standard.

2.7 Designing of parts

Designing of parts are done using Abaqus Standard. Abaqus provide a variety of options to design discrete rigid, deformable, analytical rigid and eulerian types of element in geometry with modelling space of 2D, 3D and axisymmetric. Abaqus is restricted to combine rigid

elements, deformable and analytical surfaces in one part. Specification of one particular element type results the whole part to be rigid or deformable. The deep drawing model was made by using rigid and deformable parts.

A rigid body comprises of nodes, element or surface. The motion can be controlled by allocating a reference node along single node of body. During simulation, the position of all other nodes of a part remains constant with respect to reference node (see Figure 11). The contribution of mass and inertia of elements can be specified according to requirement of problem. Properties allowed to rigid body are mass, rotary inertia, spring, dashpot and heat capacity.

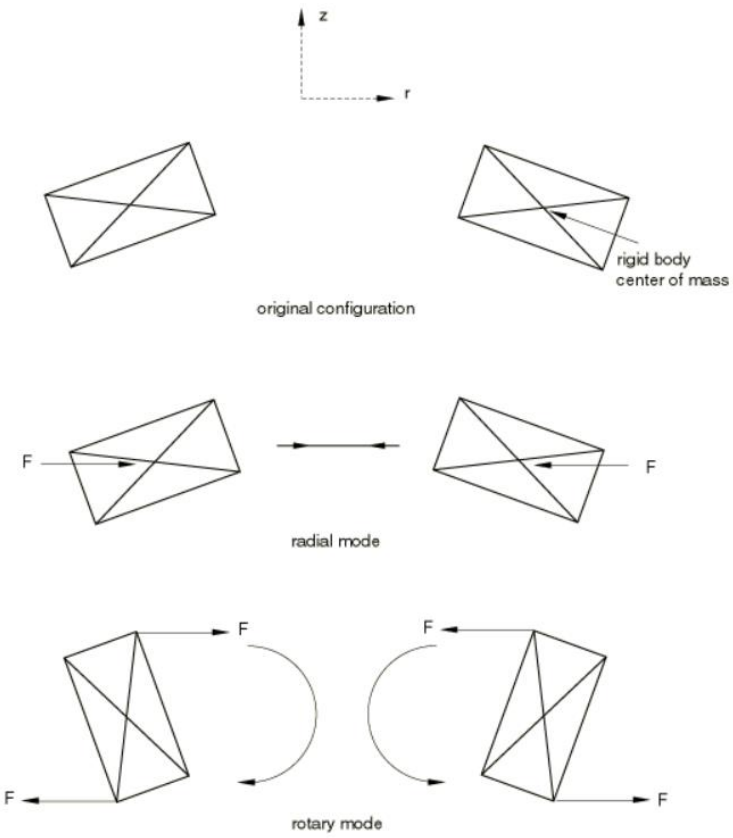

Figure 11. Motion configuration of rigid body.

Analytical rigid part behave similar to discrete part. The shape of analytical rigid is not based on arbitrary options but restricted to sketch lines, arcs and parabolas. On the other hand, deformable part can be shaped as axisymmetric, 2-D and 3-D part. Abaqus also provide flexibility to import part from other CAD software. In default, it creates deformable part that

can deform under different loading conditions. Load can be mechanical, thermal or electrical depend on problem defined.

In this thesis, only one quarter of assembly is designed and simulated because of symmetry. It also reduces the simulation time and enhance precision and accuracy in results.

2.7.1 Male die

Male die was made by using discrete rigid type elements with a reference node (RP1) to control motion. It was a shell surface, hollow from inside. Dimensions (see Table 3) were extracted from deformed tray package. It include features of extrude, extrude cut, draft angle, round, remove cell and reference point.

Table 3. Dimensions of male die.

Features	Values (mm)
Length	122.5
Width	71
Depth	38
Round 1	30
Round 2	4.56
Draft angle	103

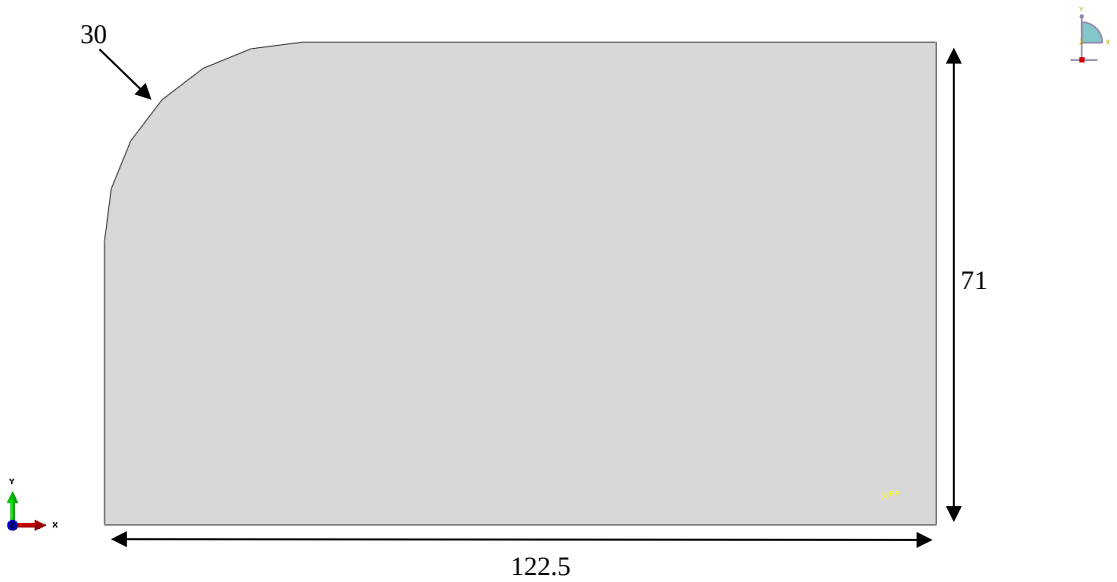

Figure 12. Top view of male die.

Figure 13. Side view of male die.

Figure 14. 3-dimensional view of male die.

2.7.2 Female die

Like male die, female die was also made from discrete rigid type with reference node (RP2). It has shell structure. Features included were extrude, extrude cut, draft angle, round, remove cell and reference point (see Figure 21).

Table 4. Dimensions of female die.

Features	Values (mm)
Length	122.94
Length	160
Width 1	110
Width 2	71.44
Round 1	30.44
Round 2	5
Draft angle	103
Depth	40

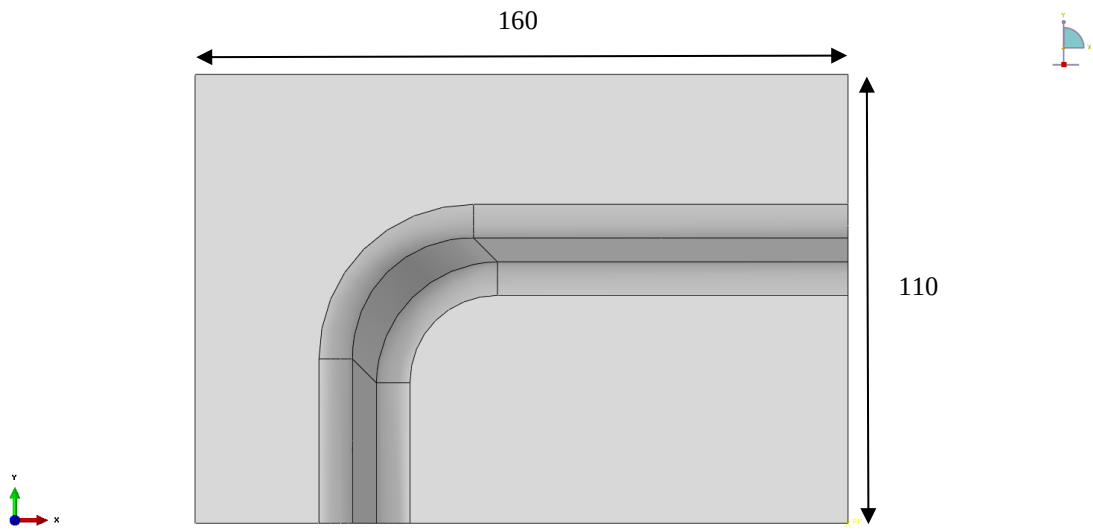

Figure 15. Top view of female die.

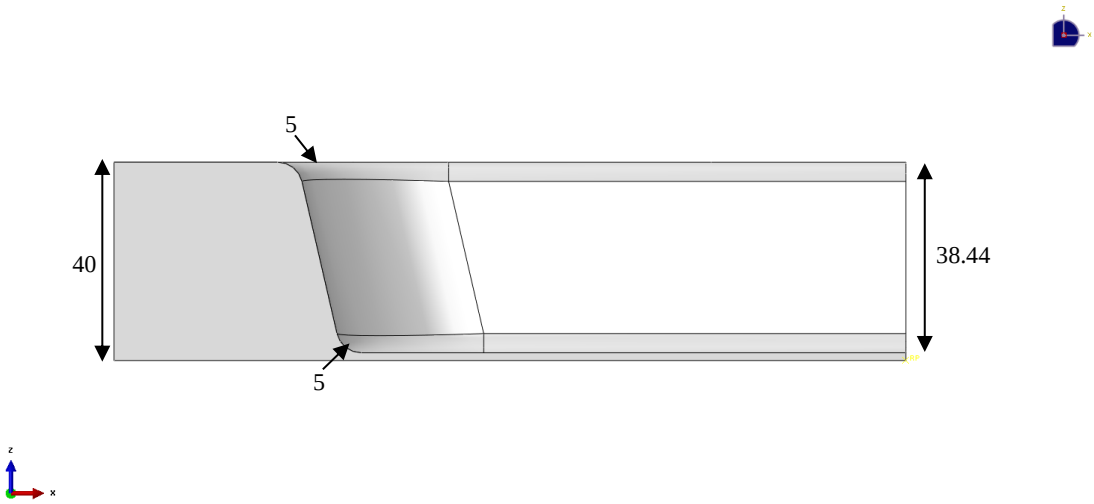

Figure 16. Side view of female die.

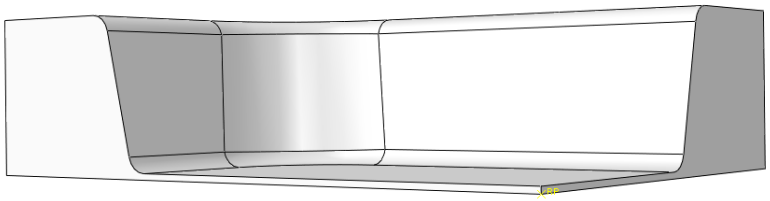

Figure 17. 3-D view of female die.

2.7.3 Blank holder

Blank holder also belonged to discrete rigid family with reference point RP3. It controls the defect during forming and provide releasing force for edges convertibility. It included features of extrusion, remove cell and round. It has similar dimension (see Table 5).

Table 5. Dimensions of quarter of blank holder.

Features	Values (mm)
Length	37.5
Length	160

Table 5 continues. Dimensions of quarter of blank holder.

Features	Values (mm)
Width	110
Width	38.56
Round	30.44
Depth	3

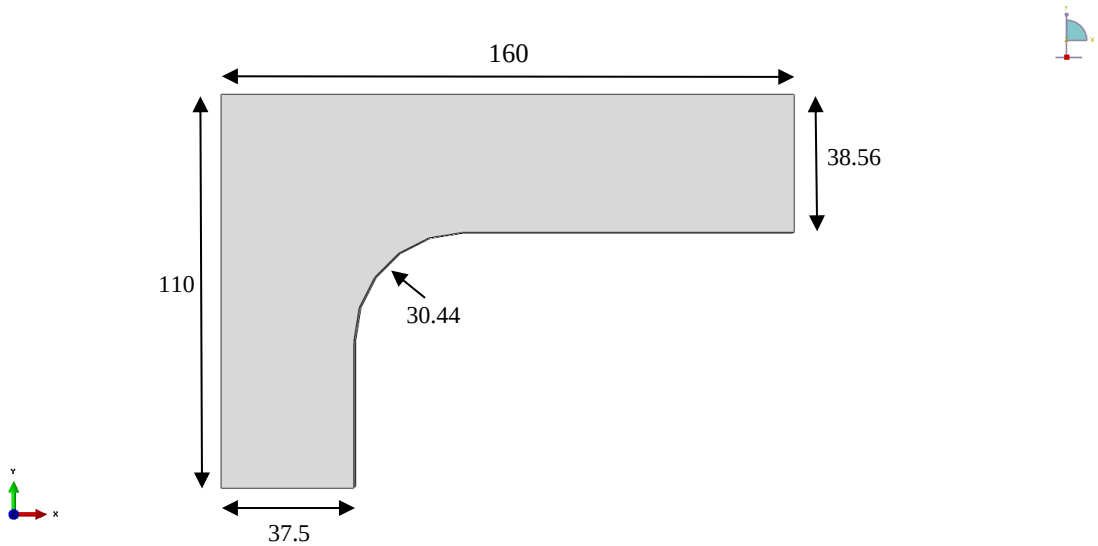

Figure 18. Top view of blank holder.

Figure 19. 3D view of blank holder.

2.7.4 Paperboard

Single ply paperboard was modelled with thickness of 0.44 mm. It was made by using deformable material. Lappeenranta University of technology (LUT) flexible packaging laboratory provided the dimensions of paperboard tray package and paperboard material was provided by Stora Enso Imatra.

Table 6. Dimension of paperboard.

Features	Values (mm)
Length	319.30
Width	216.30
Thickness	0.44
Radius	69.7203

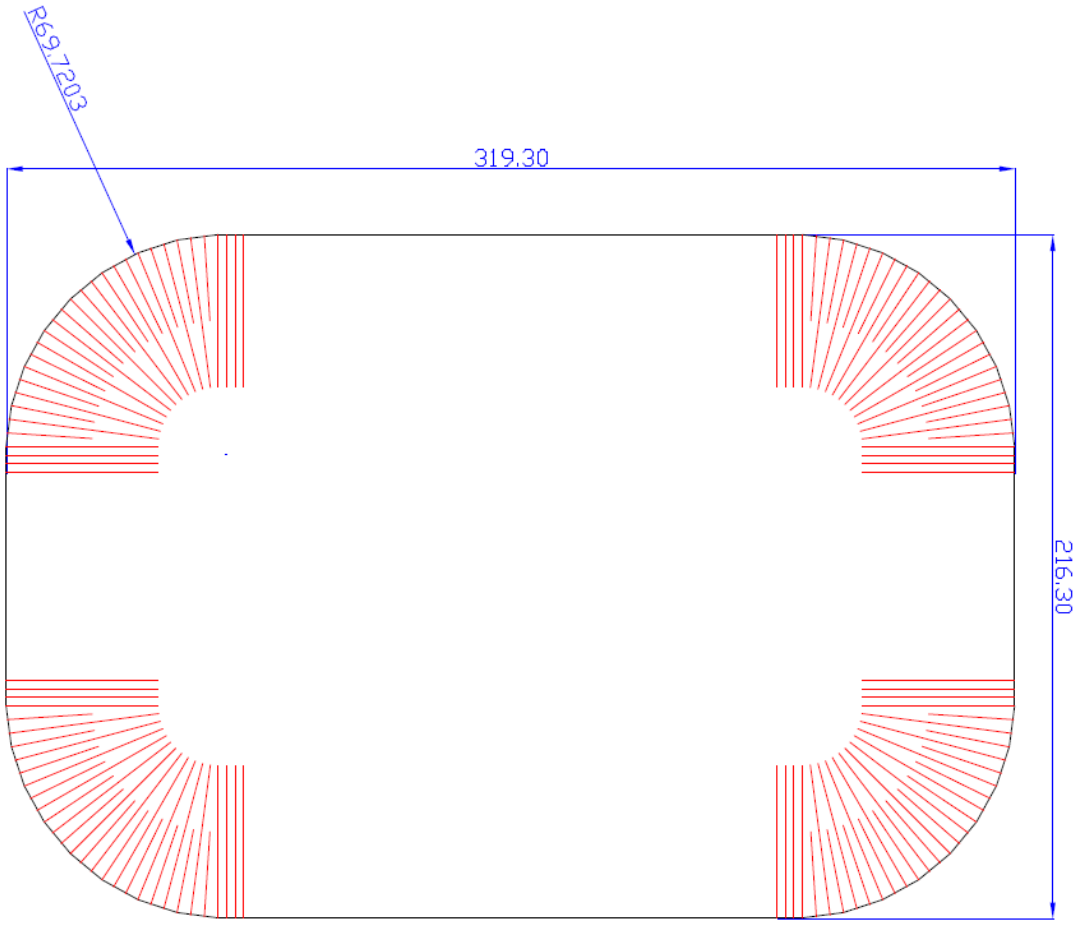

Figure 20. Dimension of paperboard tray (before forming).

Only one quarter of paperboard was modelled by Abaqus. The dimensions (as Table 7) of plane paperboard (see Figure 21) are as

Table 7. Dimensions of one quarter of plane paperboard.

Features	Values (mm)
Length	159.65
Width	108.15
Thickness	0.44
Radius	69.7203

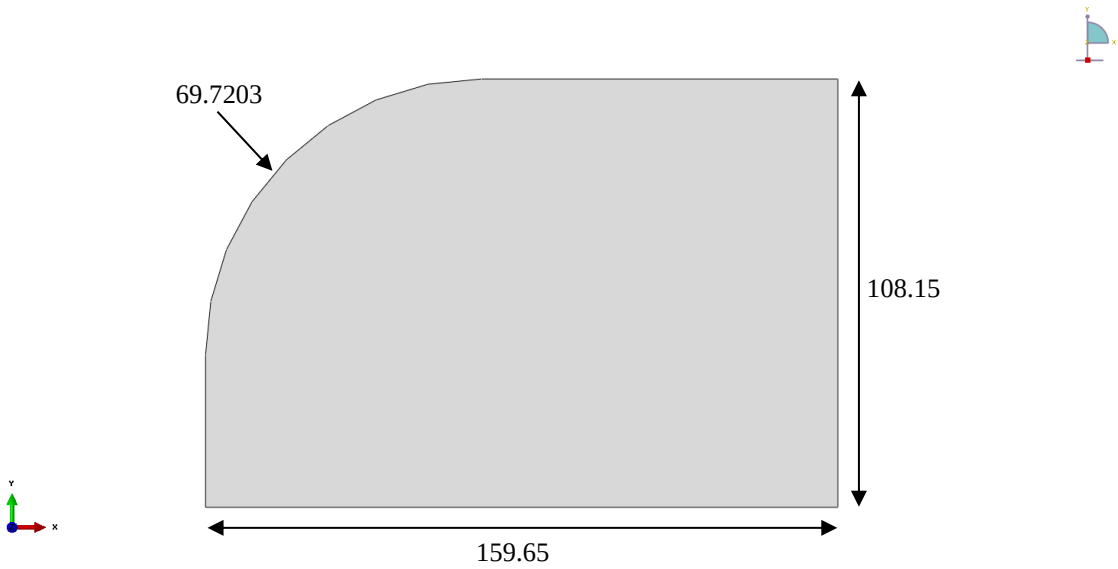

Figure 21. Model of paperboard.

2.7.5 Tray package

All the dimension were extracted from end product geometry. The CAD drawing of part was made by LUT flexible packaging laboratory.

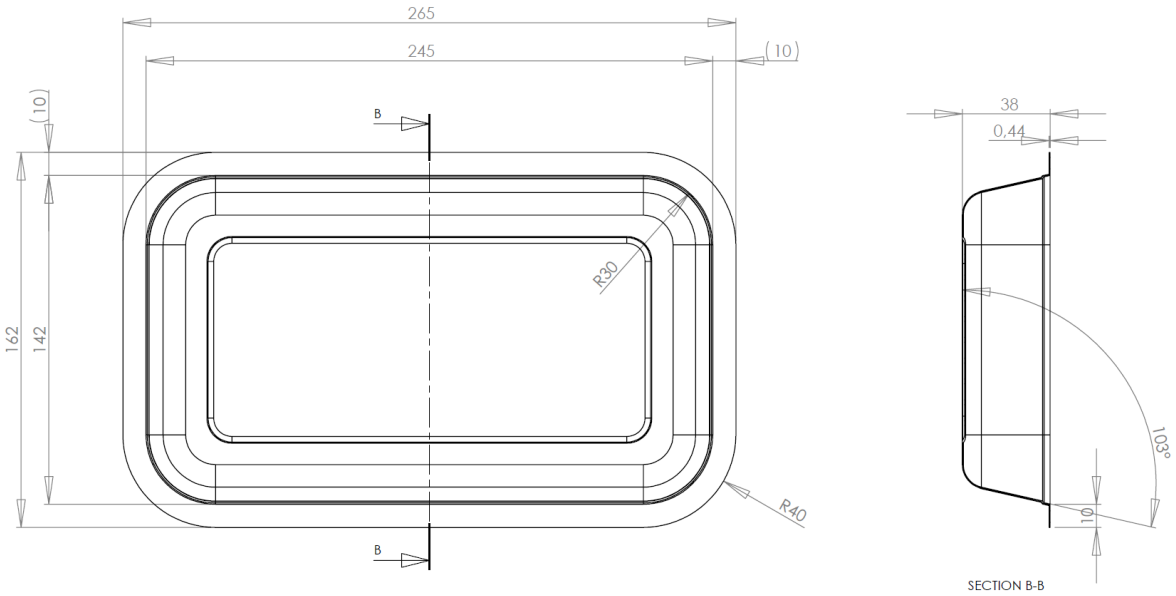

Figure 22. Drawing of paperboard tray package.

2.8 Material orientation

As paperboard is highly anisotropic material. Material orientation is a critical parameter in order to compile accurate results. Paperboard deformation based on directional properties. In modelling, direction 1 (blue) correspond to MD, direction 2 represents (yellow) CD and direction 3 (red) as z-direction (see Figure 23).

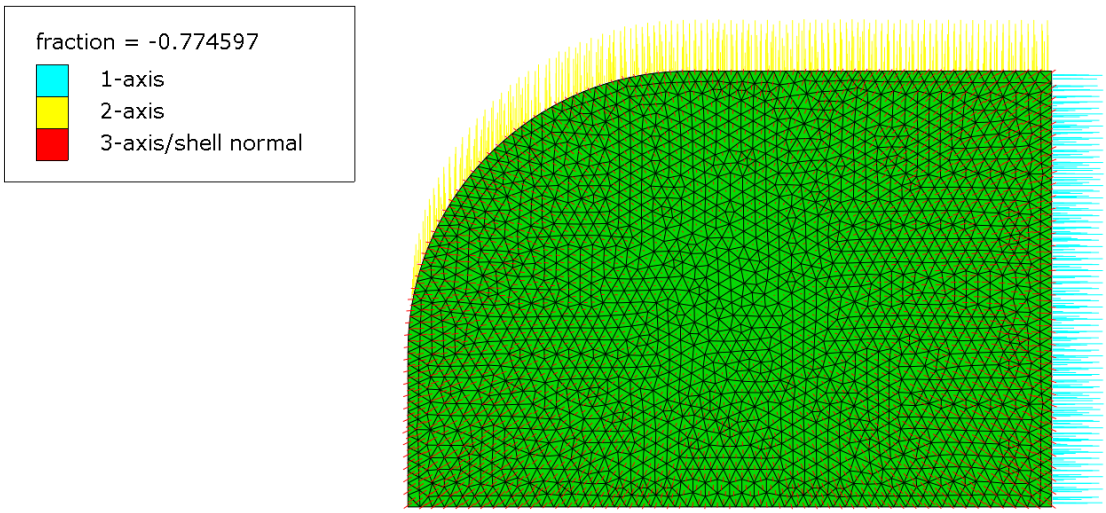

Figure 23. Material orientation

2.9 Meshing

Abaqus provides mesh tool to divide the parts or assemblies into finite number of elements and nodes with specified element type. To meet the requirement of problem, it provide variety of mesh control options. Mesh attributes can be assign to part or assembly such as element type, seeds and different meshing techniques-bottom up for complex geometry. Mesh can be modified and regenerate easily. Following features can be attained by using mesh module

- Mesh density can manually set with respect to local and global level.
- Assigning different colors to the model comprise of complex geometry and mesh technique.
- Mesh control provide flexibility in element shape, structure, technique, algorithm and adaptive remeshing rules.
- The assignment of element type and creation of part as an orphan mesh.
- Mesh verification tool to create a quality mesh part.
- Mesh density along the edges or intricate corners can be controlled by seeding mesh option.

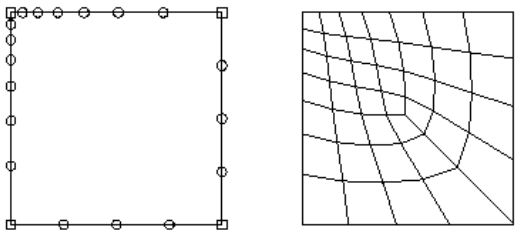

Figure 24. A model with biased seeding.

2.9.1 Element type

Mesh element type controls the element shape that helps in convergence of solution. Right element type reduces the analysis type and enhance accuracy. Abaqus provide variety of element types.

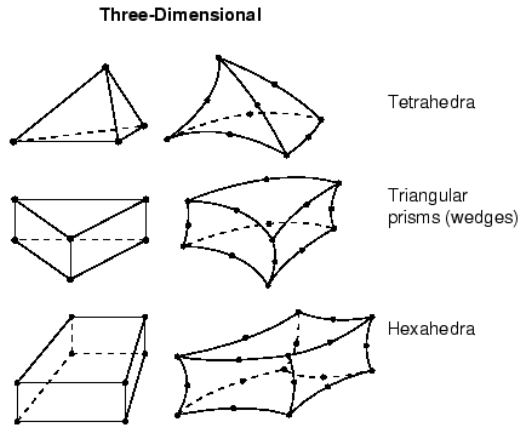

Figure 25. Element types and shapes.

Paperboard is interpreted by planner shell surface with specific thickness values. In case of two dimensional geometry, triangular and quadrilateral element types are available. Topologically these shapes are equivalent to linear quadrilateral but specific for analysis type such as CPE4 (4-node bilinear plane strain quadrilateral, reduced integration, hourglass control), c and S4R (4-node doubly curved shell, reduced integration, hourglass control, finite membrane strains) are consider to deal with stress analysis, AC2D4 (4-node linear 2-D acoustic quadrilateral, reduced integration, hourglass control) can measure acoustic analysis.

Abaqus by default allocate certain element type to mesh region. The element shape is relate by its characteristics of element type such as shell part after meshing, assigned by triangular and quadrilateral element type as an auto generated tool in Abaqus. Element type of mesh region can be interpreted by equivalent element shape. For example, mesh region of shell can form triangular elements while ignoring the quadrilateral element type.

The analysis of problem also depend on element size, type and topology. Smaller the size of element, the result will be more precise and accurate. Selection of element size and type can be chosen on the basis of problem defined. Smaller element size will lead to large simulation time. In order to attain the better results within time constraint, there should be balance between element size and simulation time.

2.9.2 Tri mesh

In this thesis, paperboard was made using 2D planner shell element with triangular mesh type. The elemental size was 3mm. Triangular mesh control is a preferred selection to analyze a solid regions of geometry.

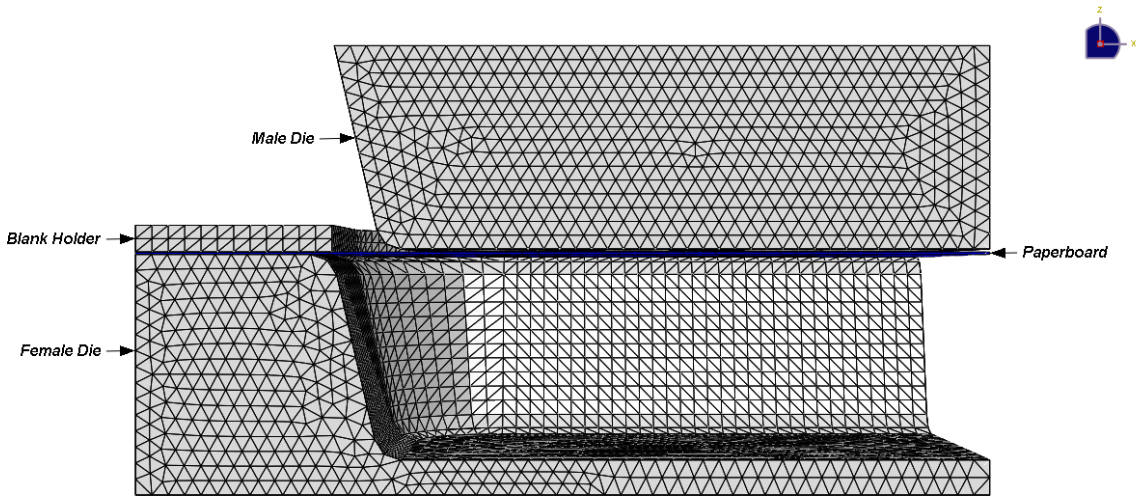

Figure 26. Tri Mesh assembly of forming tool.

2.10 Possible patterns

Currently paperboard tray package was made using linear creasing patterns (see Figure 27). It improves the bending stiffness of the round area by enhance the convertibility of paperboard and avoid tearing. Crease morphology can be enhanced by adopting different patterns such as rectangular and combination of hexagonal and pentagonal symmetry.

2.10.1 Linear crease pattern

Linear crease pattern is usually used for forming of tray package. Operation of design has been verified with converting tests held in LUT packaging laboratory. It is not only enhance convertibility of paperboard, instead it gave specific stiffness to paperboard to adopt the complex shape of die.

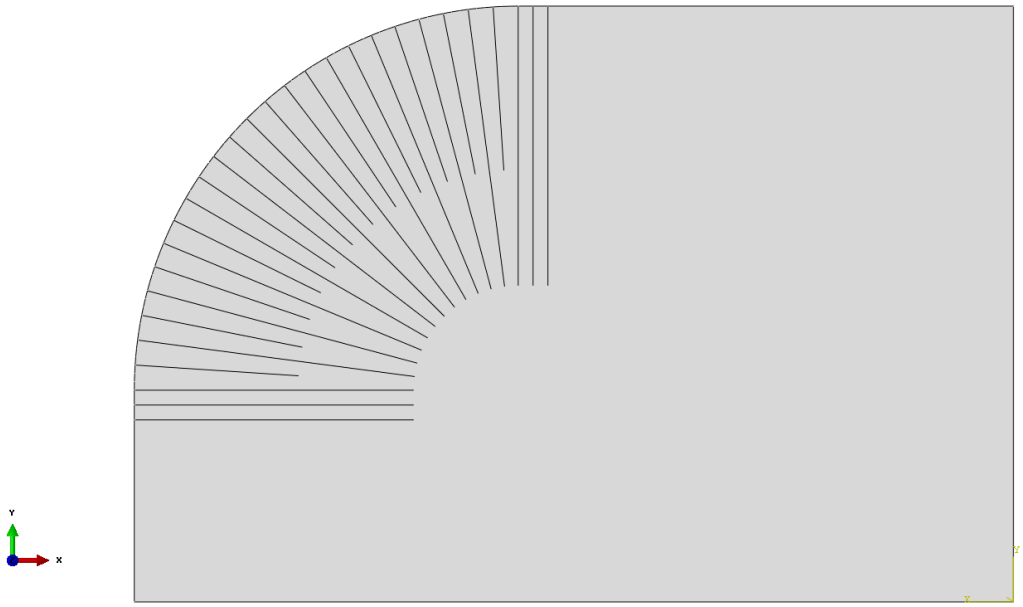

Figure 27. Linear crease pattern.

2.11 Creases

Crease can define as a separation line that distinguish two folded surfaces of paperboard. Modelling of crease is a challenging task. The degree of freedom that a crease line offer is similar to hinge joint. The working mechanism of crease line can be depicted by simple six degrees of freedom (three displacement and three rotational). To correlate the mechanism with hinge joint, rotation is allowed only along one axis and rest consider as insignificant (see Figure 36). The rotation axis act as crease line that provide rotation of 360^0.

$$u_1=0,\ u_2=0,\ u_3=0,\ ur_1=0\ ur_2 \neq 0\ \&\ ur_3=0$$

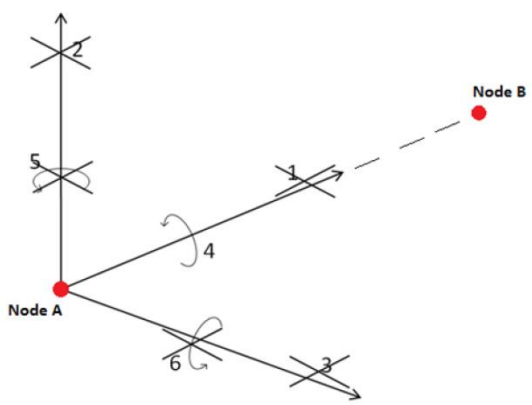

Figure 28. Degrees of freedom illustration (Amigo 2012, p. 11).

However, hinge joint allow the motion of corresponding connected nodes along x, y and z axis (see Figure 28). The working mechanism and performance solely dependent on material properties (elastic and plastic), fold angle and operating geometry.

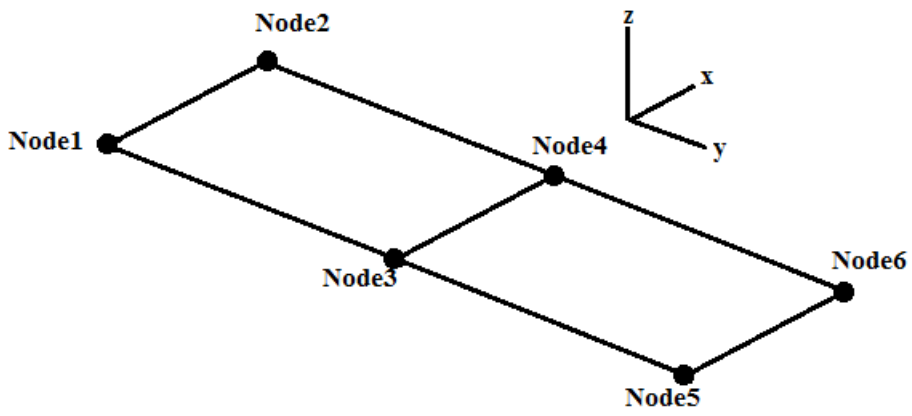

Figure 29. Linear displacement of connected nodes

In Abaqus, CONNECTOR tool provide the option to achieve required degree of freedom by simply using hinge joint that connect two nodes and restrict five degrees of freedom and allow only rotation along crease line (see Figure 29). It set conditions between two nodes, that are usually parallel but allow joint to move along x, y and z direction. This is the closest way to correlate crease behavior with actual folding of paperboard; to maintain proper bending stiffness of material. Crease performance depend on number of factor such as bending stiffness, crease angle, tensile properties of paperboard and geometrical complexity of part.

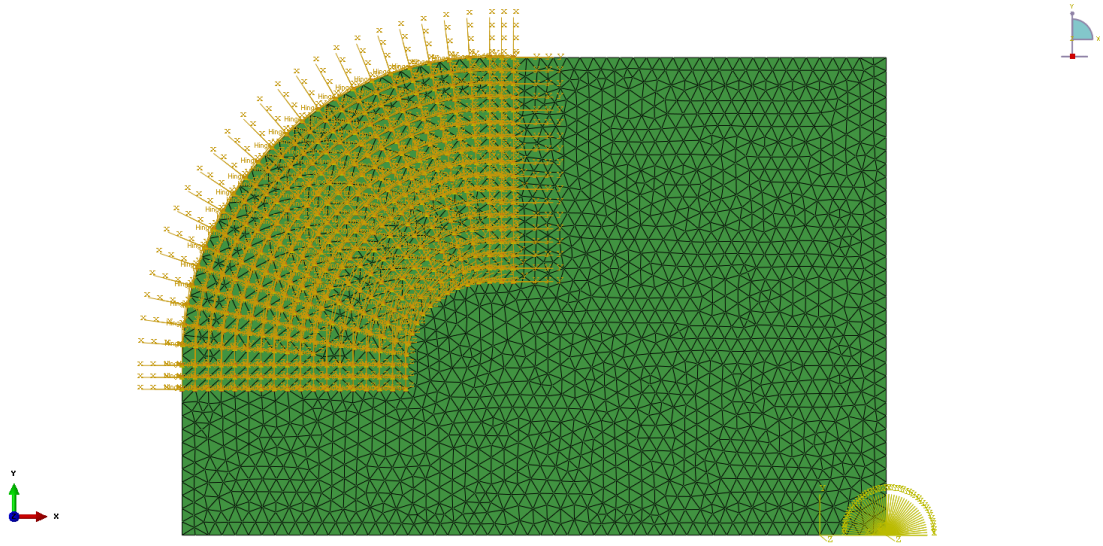

Figure 30. Model of creases on paperboard.

2.12 Boundary conditions

Boundary conditions are the base of proper working of assembly. It restrict the parts to compute in specific dimensions (see Table 9). It include loads and displacement of male die, female die, blank holder and paperboard (see Figure 40). The boundary conditions used to define the mechanism of forming is presented in table 9.

Table 9. Boundary conditions.

Parts	Type	Boundary conditions
Male Die	Displacement/Rotation	U_1= 0 U_2= 0 U_3= -38 mm UR_1=0 UR_2=0 UR_3=0
Female Die	Displacement/Rotation	U_1= 0 U_2= 0 U_3= 0 UR_1=0 UR_2=0 UR_3=0

Table 9 continues. Boundary conditions.

Parts	Type	Boundary conditions
Blank Holder	Displacement/Rotation	U_1= 0 U_2= 0 $U_3 \neq 0$ UR_1=0 UR_2=0 UR_3=0
Paperboard	Symmetric/Antisymmetric	Along x axis edge YSYMM U_2=UR_1=UR_3=0 Along y axis edge XSYMM U_1=UR_2=UR_3=0

Concentrated force compel the blank holder to move downward and act as blank holding force. It avoid the paperboard from wrinkling. In reality, first blank holder moves along downward direction and after particular units of displacement of male die, it move upward to allow material to adopt complex shape.

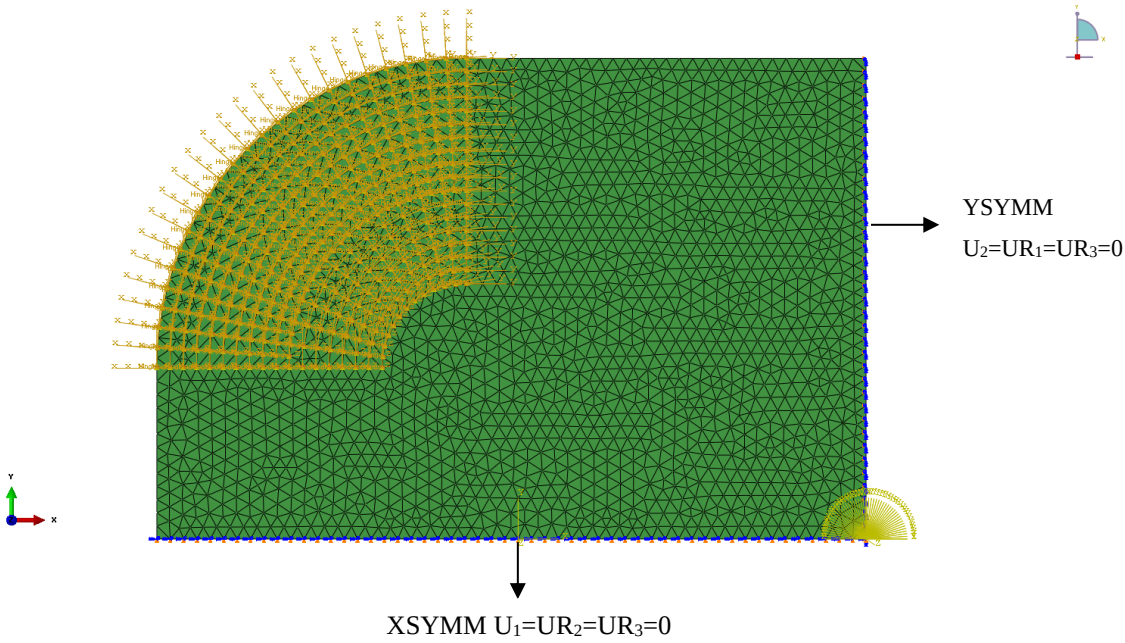

Figure 31. Boundary condition of paperboard

2.13 Interaction

Modelling of complex geometries require contact algorithms control to achieve cost effective solution. In Abaqus, surface to surface interaction is a tool from interaction module that allows a contact between deformable surfaces or between deformable and discrete bodies. It include master and slave surface. In computational forming of paperboard, discrete parts such as male die and female die were considered as master surfaces. On the other hand, paperboard top and bottom surface behaved as slave surface (see Figure 32). A discrete region can only act as master surface, it cannot behave as slave surface.

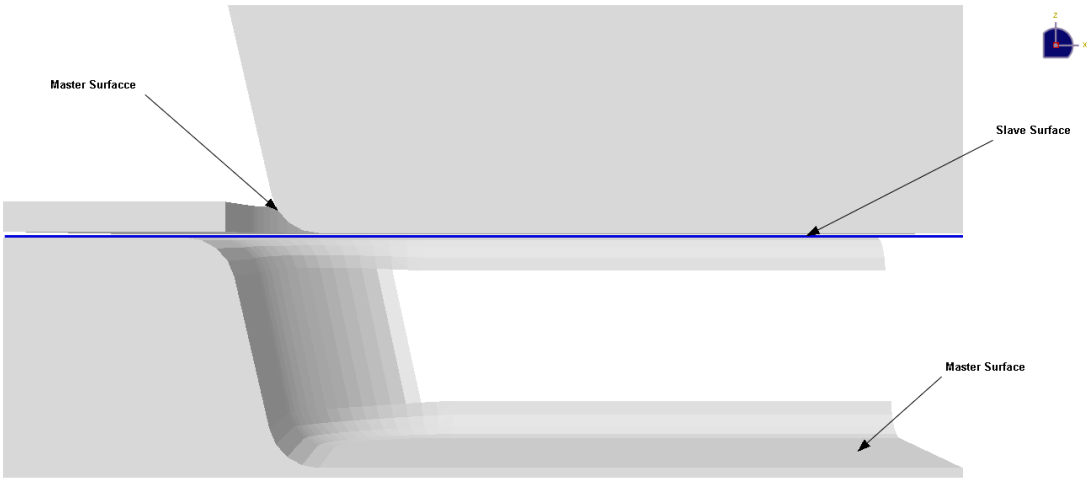

Figure 32. Master and slave surfaces in 3D forming.

2.14 Analysis

Static analysis was used in this thesis, which deals with large deformation. To deal with excessive deformation problem, NLGEOM option in Abaqus was activated. NLGEOM allowed the material orientation and rotation act together and has large deformation. It take more time to compute the solution.

3 RESULTS AND DISCUSSION

In this chapter, the experimental results obtained from previous study and simulation results obtained from paperboard forming are presented.

3.1 Experimental results

In previous study, the reaction force on male die against displacement was calculated with the help of four sensors and values were verified from novel simulation results.

3.1.1 Measurement of forming forces

In previous study, experimental calculations were carried out by advanced and precise monitoring system and series of tests on paperboard (Sulphate pulp + PET coated). Four pressure sensors were used to measure reactional force on male die against pressing depth. The curve express the behavior of substrate under influences of stresses provided by male die. (Tanninen 2015, p. 63.)

As paperboard is of symmetrical geometry, 4 sensors represents the identical behavior of curve that confirm the force distribution across the blank and displacement (see Figure 33). A single sensor was used to measure the cumulative effect of forces recoding evenly distribution. It illustrate the sharp increase in magnitude of force at first, then a stable trend in between the depth of 15 to 37 mm. A large variation in trend of each curve was observed during pressing from 37 to 45 mm depth to straighten the crease assisted folds along the wall. It increases the forming and process time. (Tanninen 2015, p. 63.)

After release of paperboard tray from forming tools, the dimensions of tray increases while it cool down to its normal temperature. Spring back effect also contribute in dimension instability.

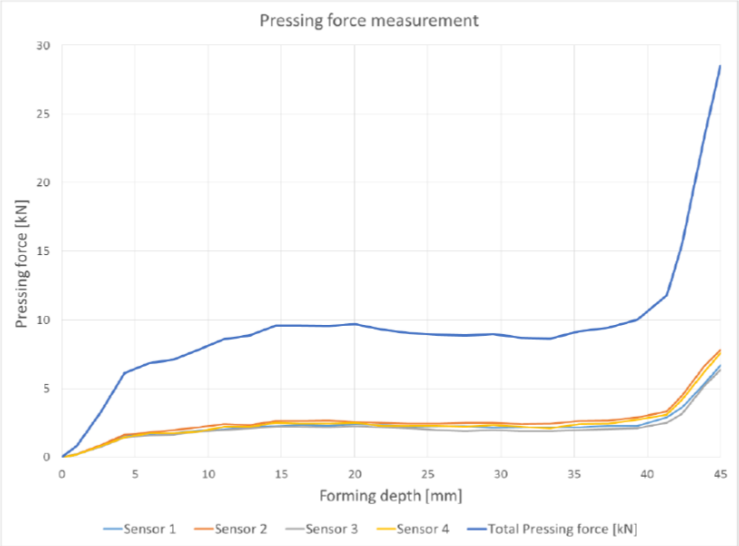

Figure 33. Force curve with respect of forming depth measured by 4 sensors (Tanninen 2015, p. 64).

During the experimentation of previous study, forming defects were also monitored. Wrinkling and rupture of blank are common defect that were detected during forming of substrate. These defects were also highlighted by simulation results. The reason behind these defects are change in process parameter and assignment of material properties (see Figure 34). (Tanninen 2015, p. 64.)

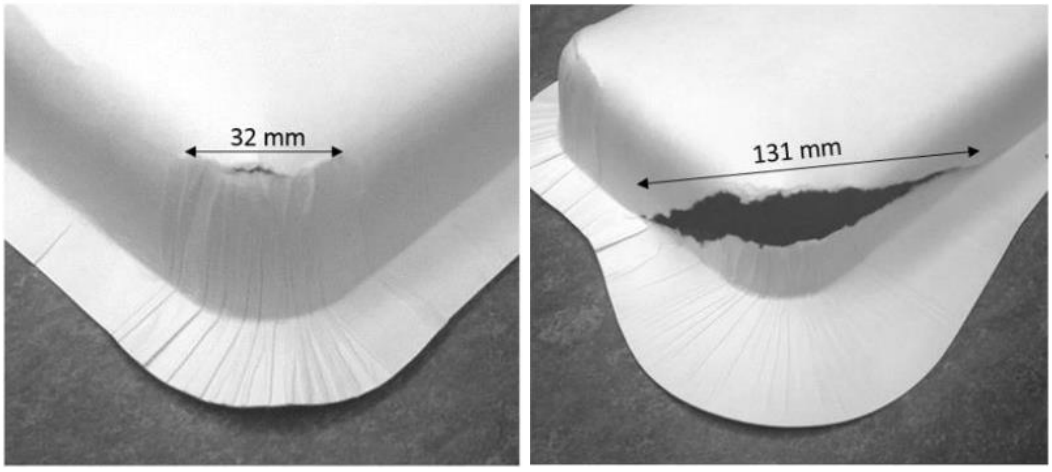

Figure 34. Defects during forming of paperboard tray (Tanninen 2015, p. 65).

The magnitude of reaction force was large because of defects (see Figure 35). The deviation of curve express the progression of forming behavior. The red arrow represents the sudden

drop of force curve, shows rupture. The cumulative force is high compared to accurate results.

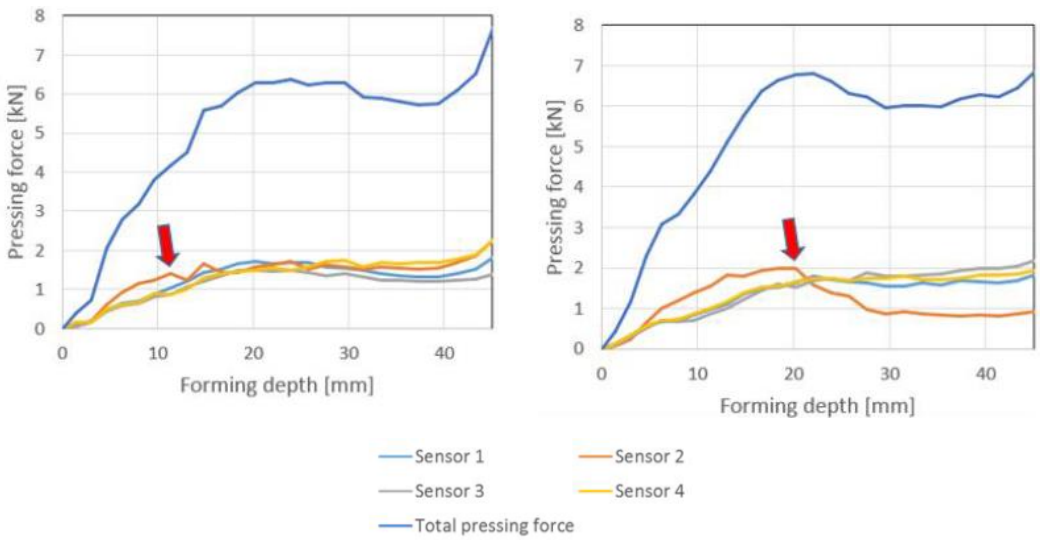

Figure 35. Performance of paperboard forming and detection of reaction force while rupturing by four sensors (Tanninen 2015, p. 65).

3.2 Simulation results

In this sub chapter, the results obtained from paperboard forming with and without the feature of creases are presented. The effect of forming on paperboard stresses and strains are analyzed. Furthermore, the reactional forces on male die was calculated and compared to experimental results.

Only one quarter of forming tools and paperboard was modelled due to the symmetry of the problem. The forming process includes three interactions: male die to paperboard, female die to paperboard and blank holder to paperboard. The interactions were assumed to be frictionless. The simulations were done using static analysis. Thermal properties of female die and spring back effect of paperboard was neglected.

The paperboard without creases was referred as the plane paperboard. Two different types of paperboard materials are analyzed, named single ply and multi-ply. Material properties are based on elastic-plastic behavior and are presented in Tables 6, 7 and 8. Paperboard was meshed by S3 shell elements type. The forming process includes excessive deformation and thus stabilization was used. The stabilization damping factor was set to 0.01.

In the simulation, male die was moved 38.5 mm into the female die, whereas blank holder was displaced 0.11mm in order to avoid wrinkling defects. Female die was fixed throughout the whole process.

3.2.1 Plane Paperboard

The total strain in MD and CD direction is calculated and presented in this section.

3.2.1.1 Total Strain

Total strain can be express as

$$\varepsilon_{total} = \varepsilon_{elastic} + \varepsilon_{plastic} \tag{16}$$

In equation 16, ε_{total} represent total strain (LE), $\varepsilon_{elastic}$ is elastic strain and $\varepsilon_{plastic}$ is plastic strain (PE).

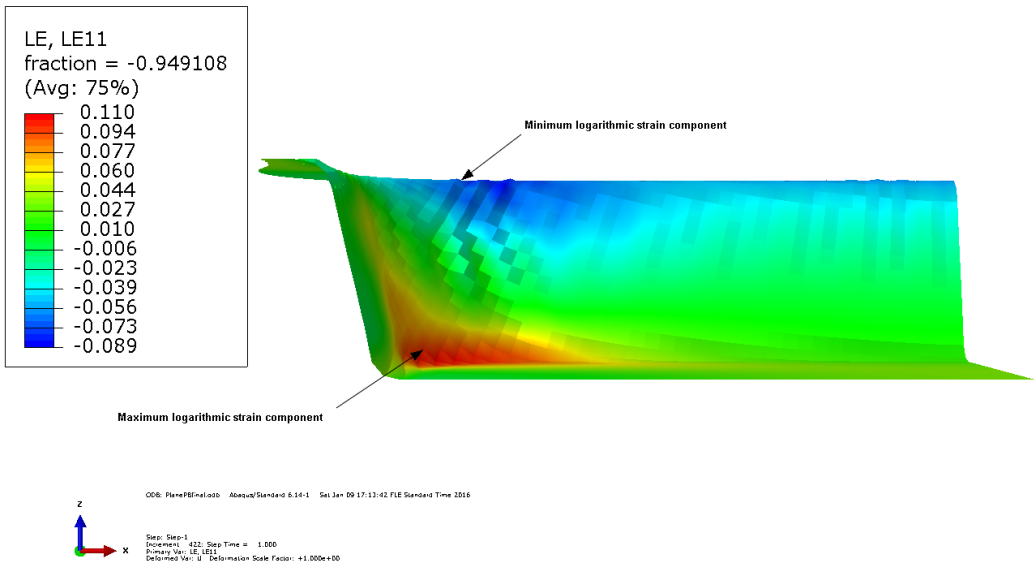

Figure 36. L11 (MD) total strain in plane paperboard.

L11 refers to total strain along MD. The blue region represent the compressional strain, the green region shows the average values of total strain within range of -0.023 to 0.044. The red region is critical, represent the maximum value (see Figure 36). The large deformation causes higher values of total strain.

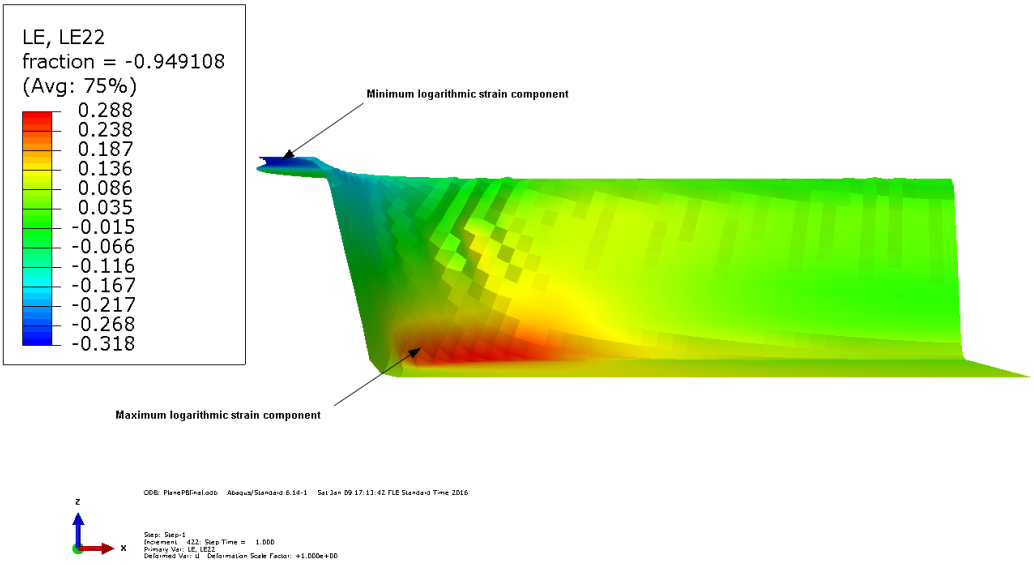

Figure 37. L22 (CD) total strain in plane paperboard.

L22 is total strain along CD. It has higher values around lower round edge (see Figure 37).

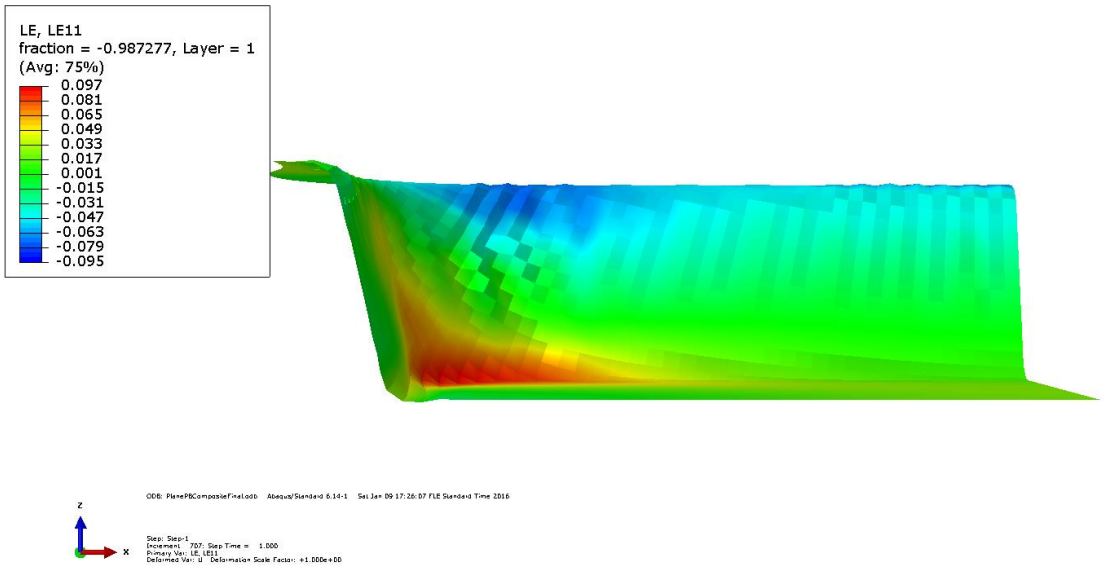

Figure 38. L11 (MD) total strain in multiply paperboard.

The difference in total strain between single ply and multiply paperboard is small with respect to its maximum and minimum values.

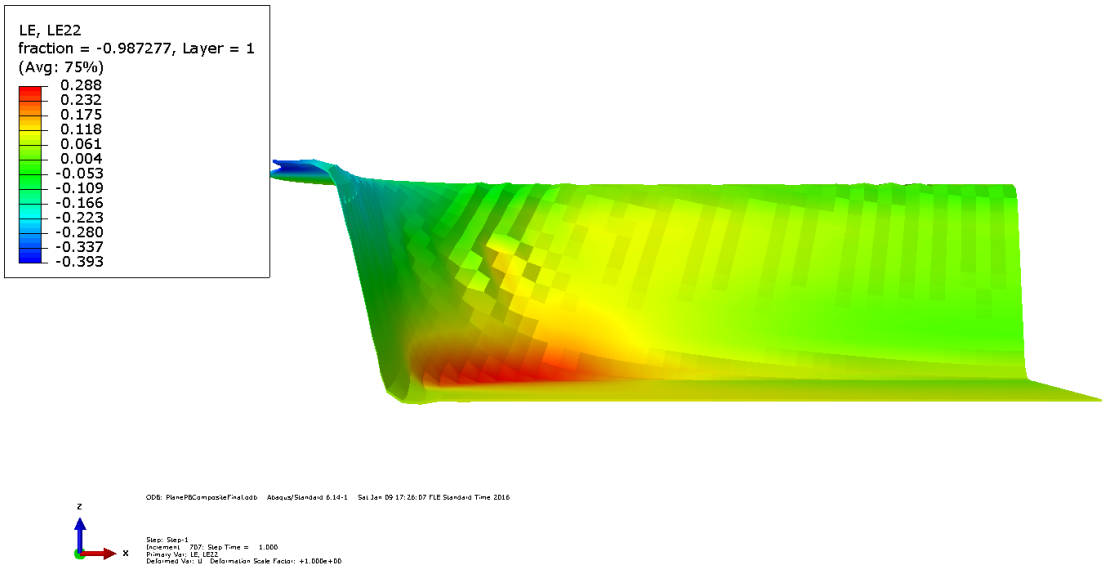

Figure 39. L22 (CD) total strain in multiply paperboard.

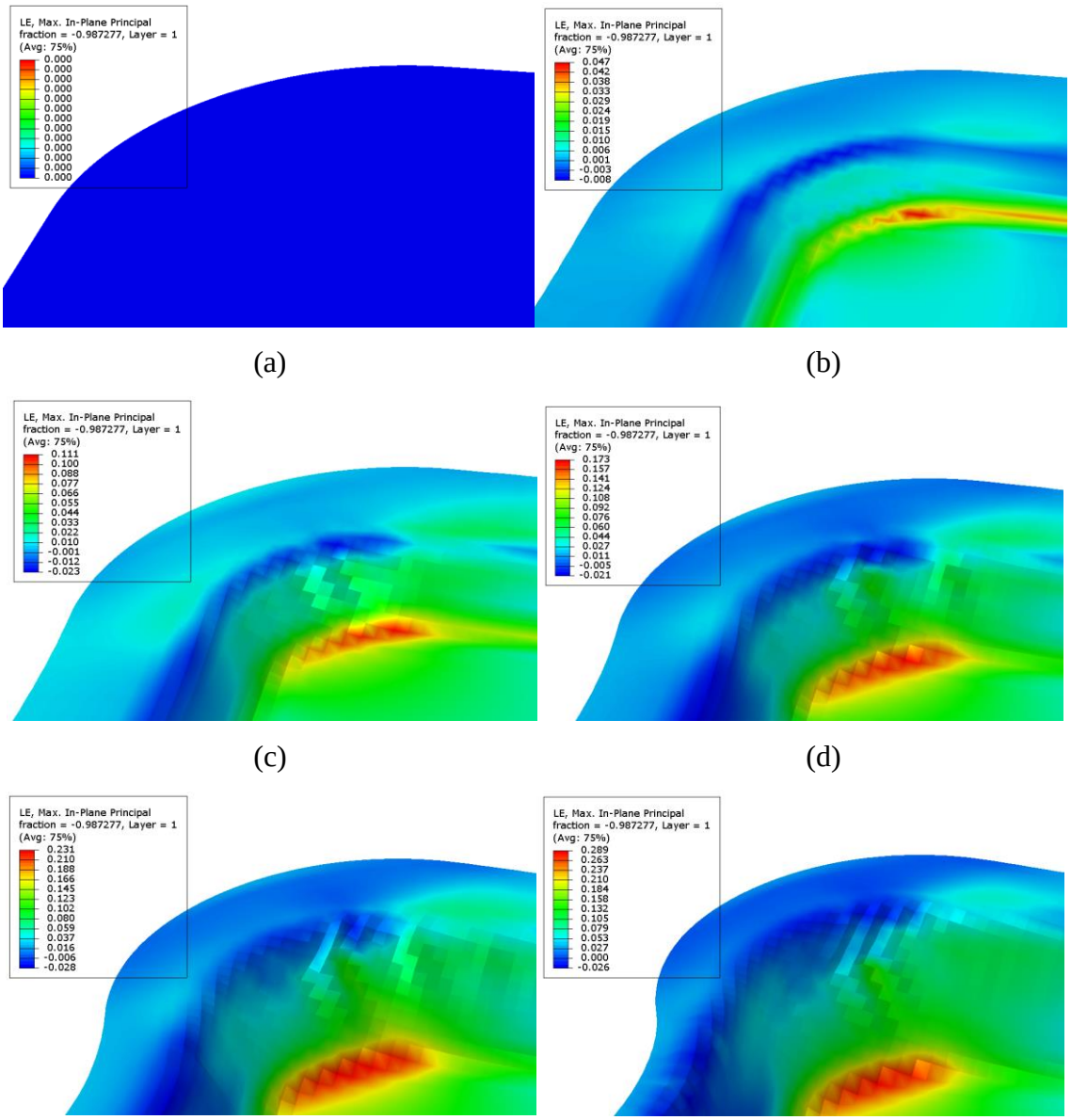

(a) (b)

(c) (d)

(e) (f)

Figure 40. Forming of paperboard tray package (Maximum In plane principal total strain). (a) Undeformed (b) 7.6mm of displacement (c) 15.2 mm of displacement (d) 22.8 mm of displacement (e) 30.4 mm of displacement (f) 38 mm of displacement.

3.2.1.2 Plastic strain

Plastic strain was followed to explain plastic behavior.

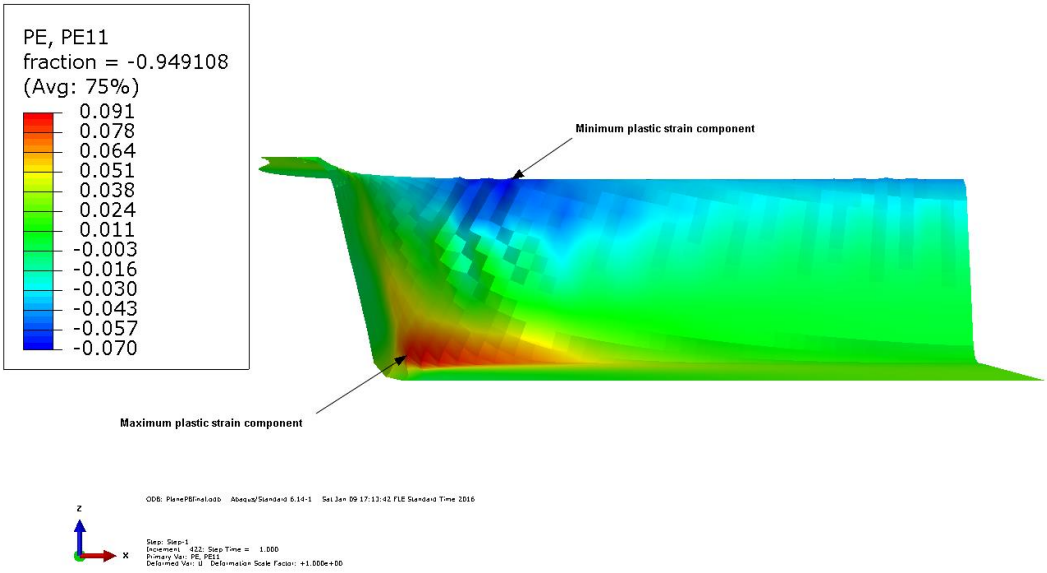

Figure 41. PE11 (MD) plastic strain in plane paperboard.

Extensional plastic strain along MD attains minimum values at green region, whereas compressional plastic strain is 7% (blue region).

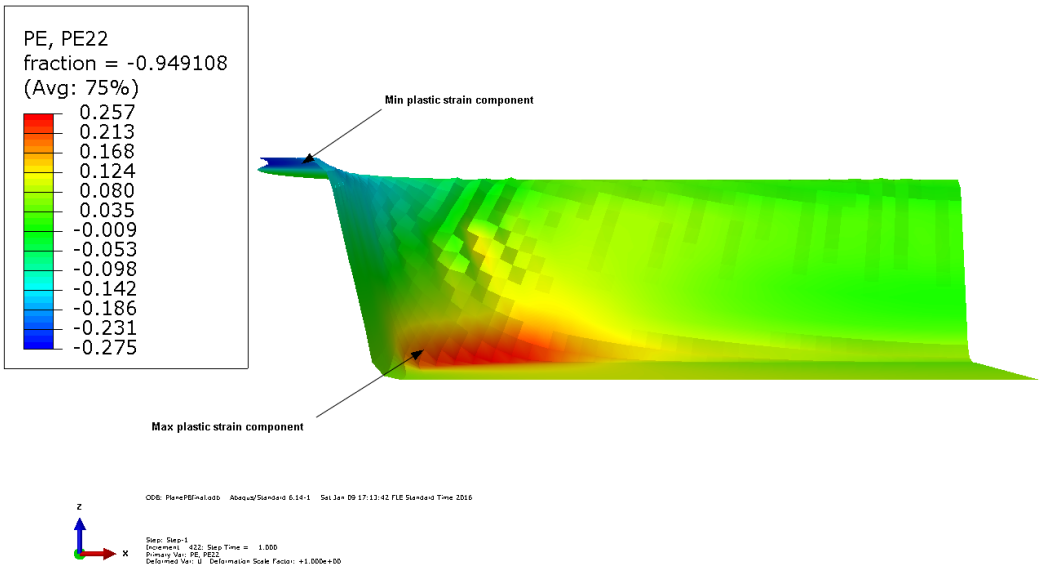

Figure 42. PE22 (CD) plastic strain in plane paperboard.

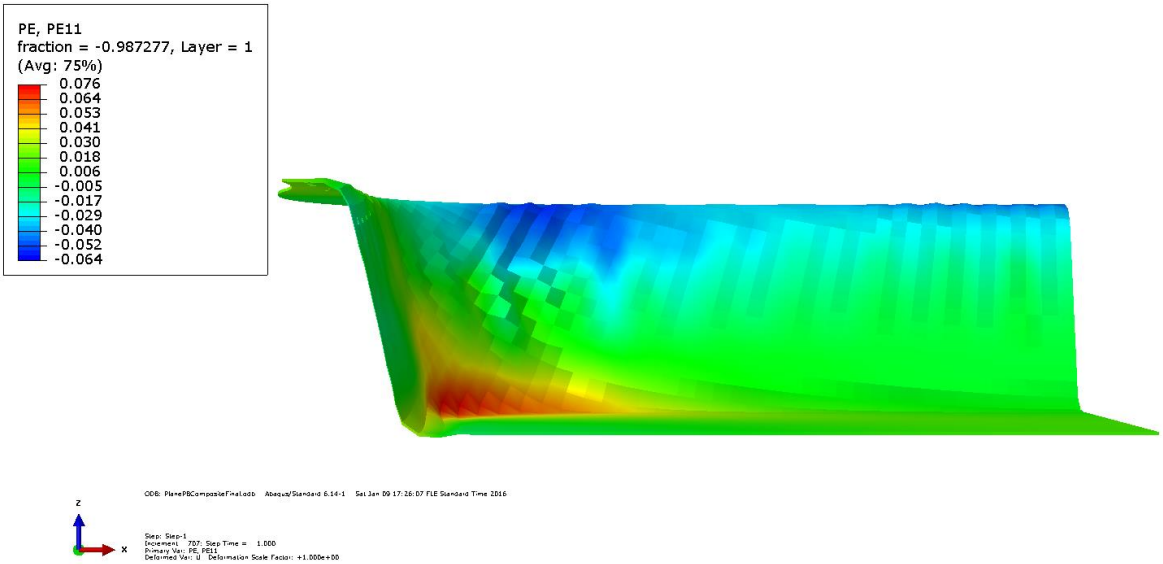

Figure 43. PE11 (MD) plastic strain in multiply paperboard.

Improvement in material model enhance the accuracy of results. The average value of plastic strain in multiply paperboard (see Figure 43), is approximately 15% less compared to single ply paperboard (see Figure 41). The plastic strain in cross direction explains the high concentration at the lower edge of formed paperboard (see Figure 44).

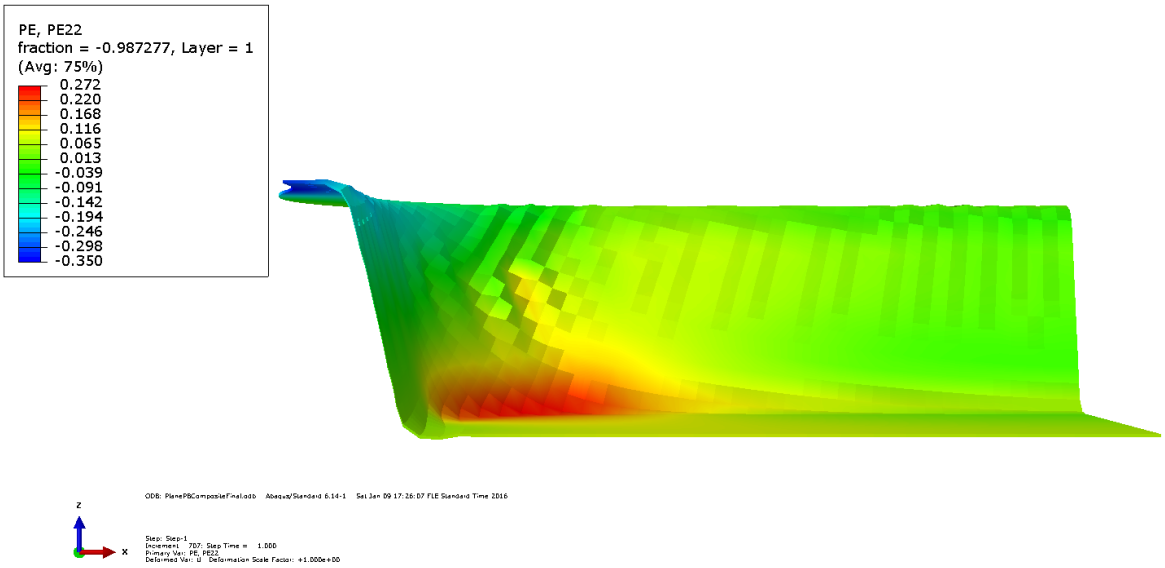

Figure 44. PE22 (CD) plastic strain in multiply paperboard.

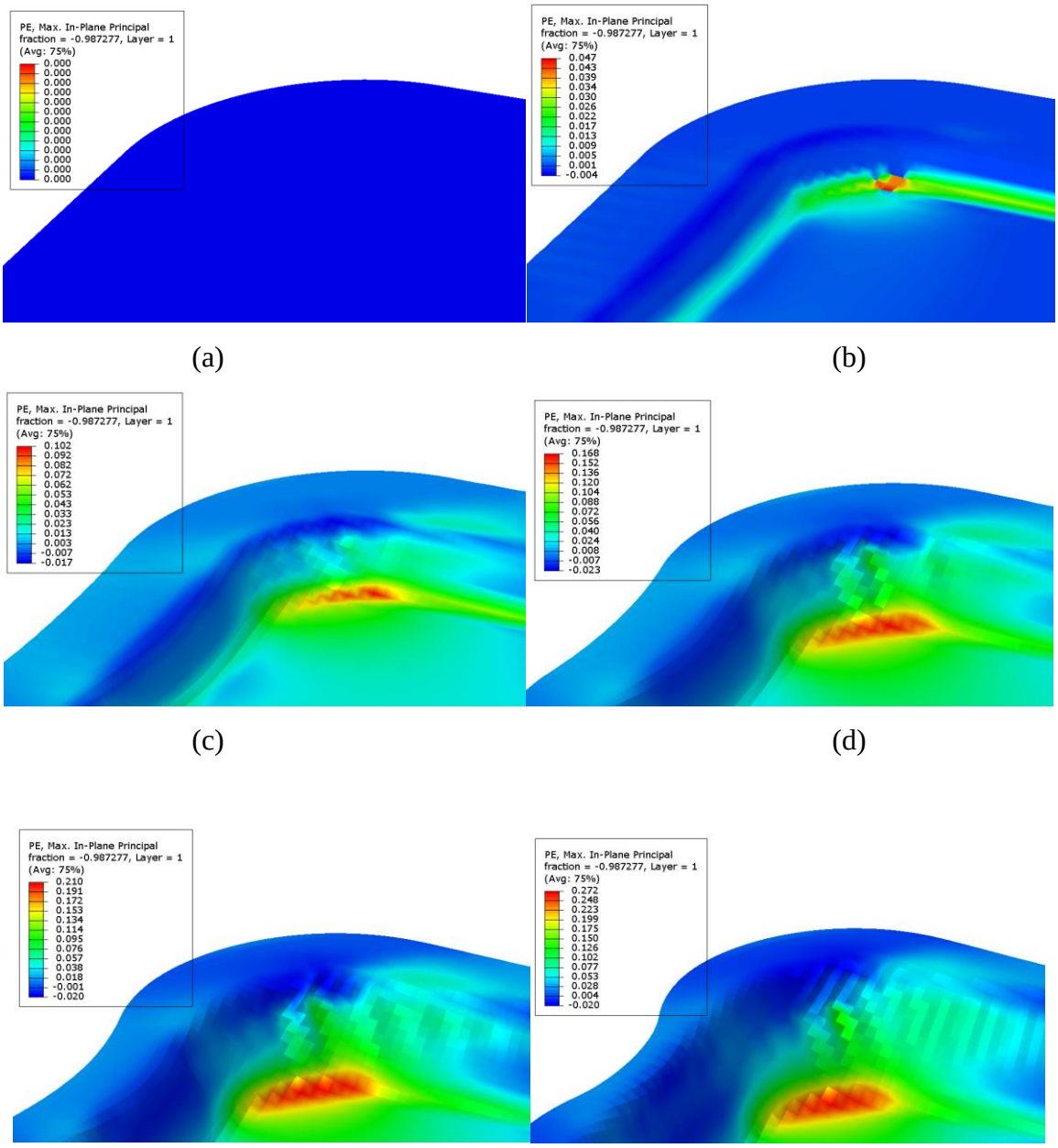

Figure 45. Forming of paperboard tray package (plastic strain). (a) Undeformed (b) 7.6mm of displacement (c) 15.2 mm of displacement (d) 22.8 mm of displacement (e) 30.4 mm of displacement (f) 38 mm of displacement.

3.2.1.3 Stresses

Stresses were analyzed during forming of paperboard. Maximum value of stress distribution was at the round edge because of geometrical complexity (see Figure 46) and (see Figure 48).

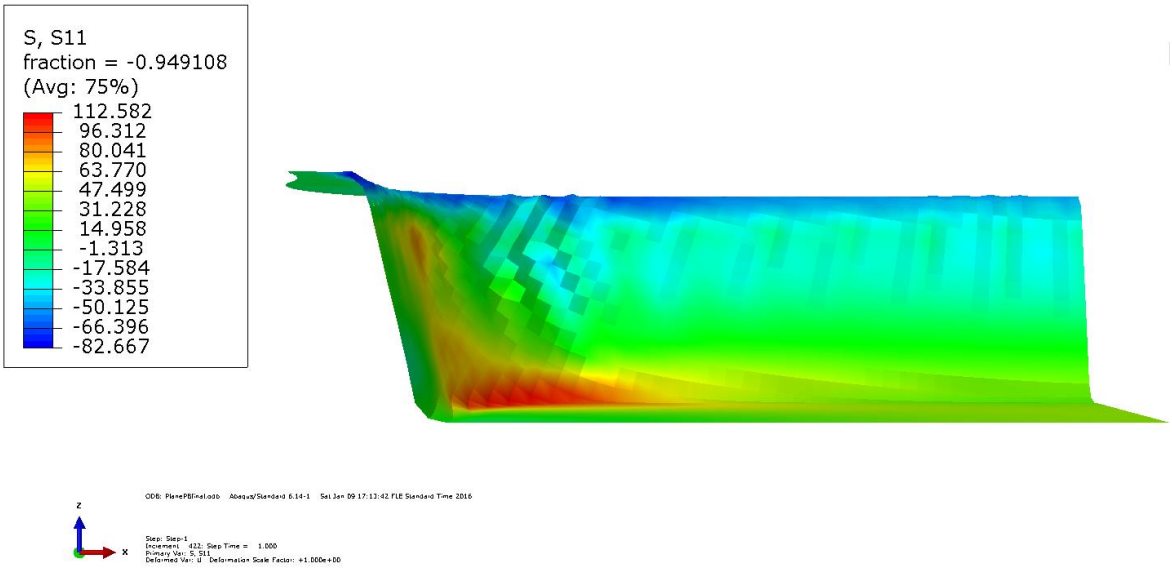

Figure 46. Stress (S11) along MD in plane paperboard.

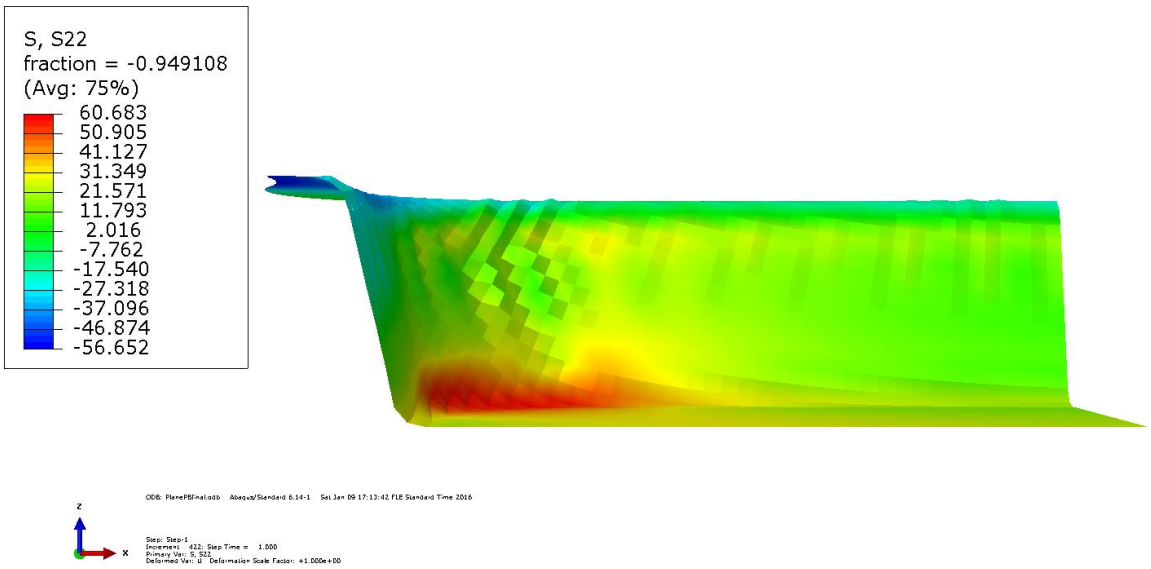

Figure 47. Stress (S22) along CD in plane paperboard.

There was a substantial change in stress calculation when paperboard material properties and structure were change to multiply. The stress was increased to 231.58 MPa from 112.58 MPa (see Figure 47) and (see Figure 49).

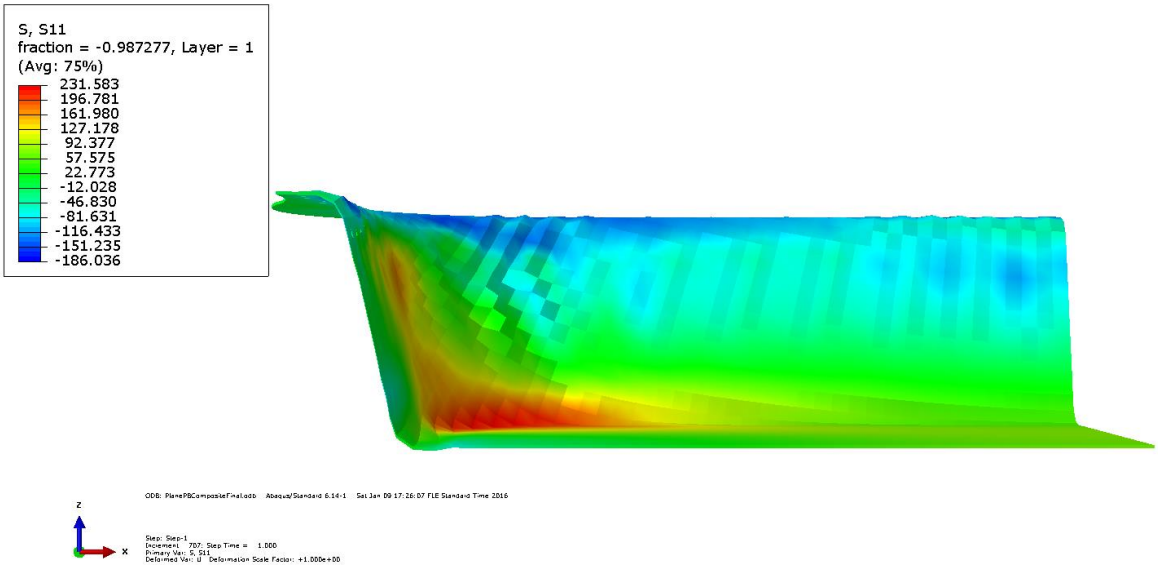

Figure 48. Stress (S11) along MD in multiply paperboard.

Stress (S22) showed different values as material properties changed from single ply to multiply (see Figure 49).

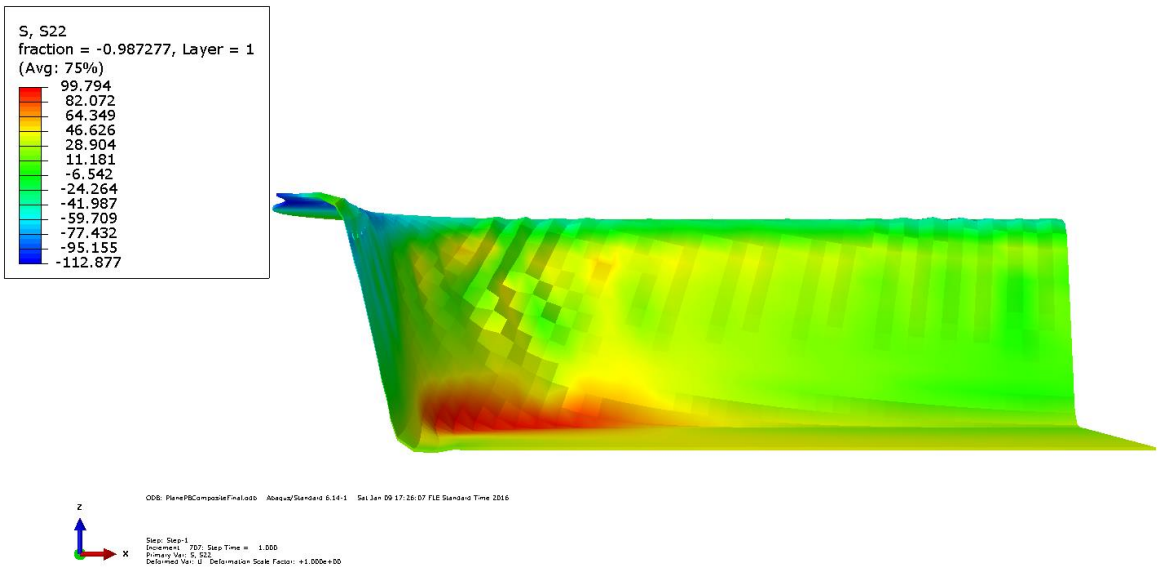

Figure 49. Stress (S22) along CD in multiply paperboard.

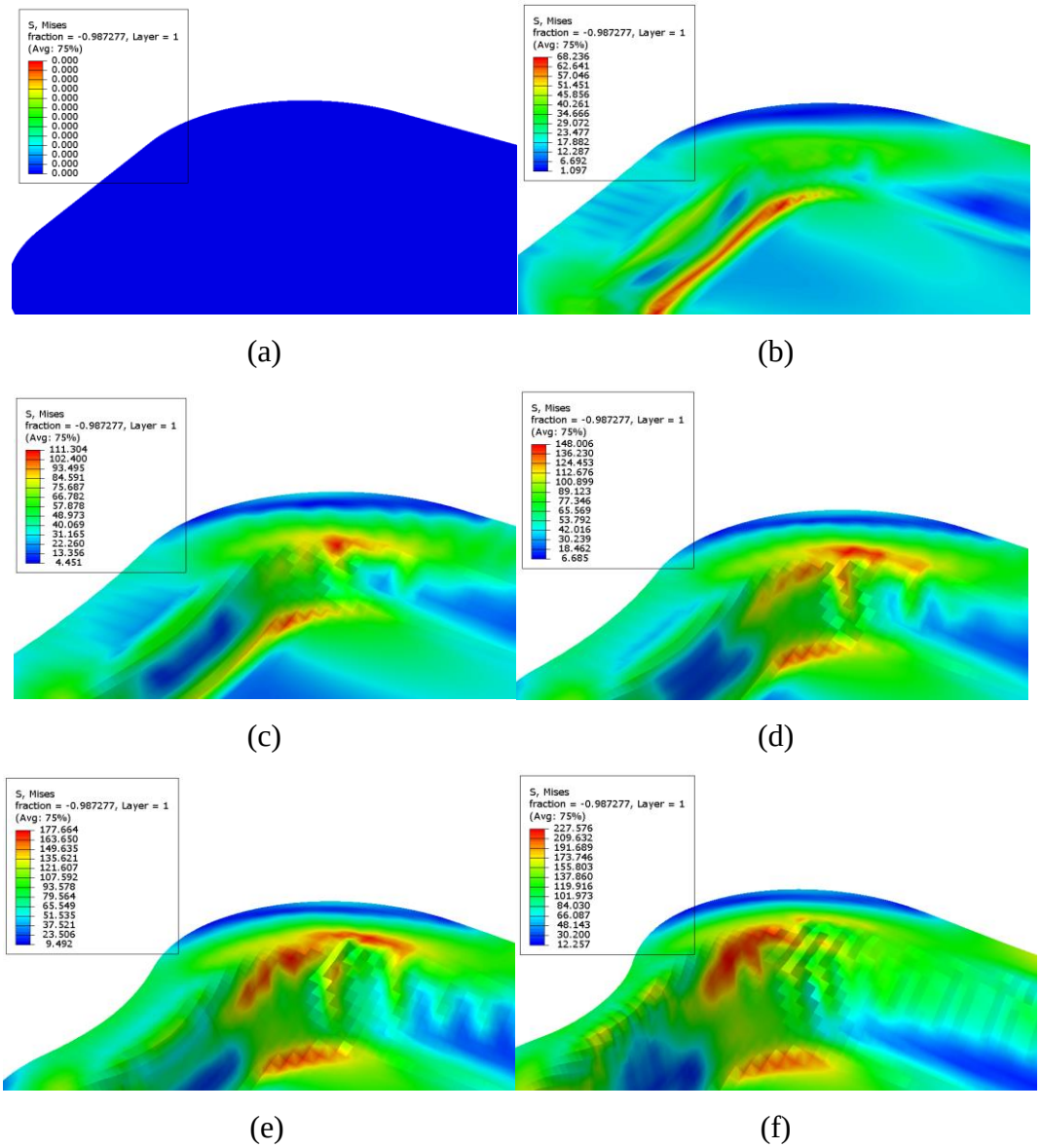

Figure 50. Forming of paperboard tray package (Von Mises stresses). (a) Undeformed (b) 7.6mm of displacement (c) 15.2 mm of displacement (d) 22.8 mm of displacement (e) 30.4 mm of displacement (f) 38 mm of displacement.

3.2.1.4 Reaction force

Reaction force on male die was calculated and plotted against displacement. The graph illustrate that the reaction force starts variation at 1.3 kN and shows stable behavior until 36 mm of displacement. At the end of the curve, a sudden increase in behavior expresses that the force required to assist the folding of paperboard (see Figure 51).

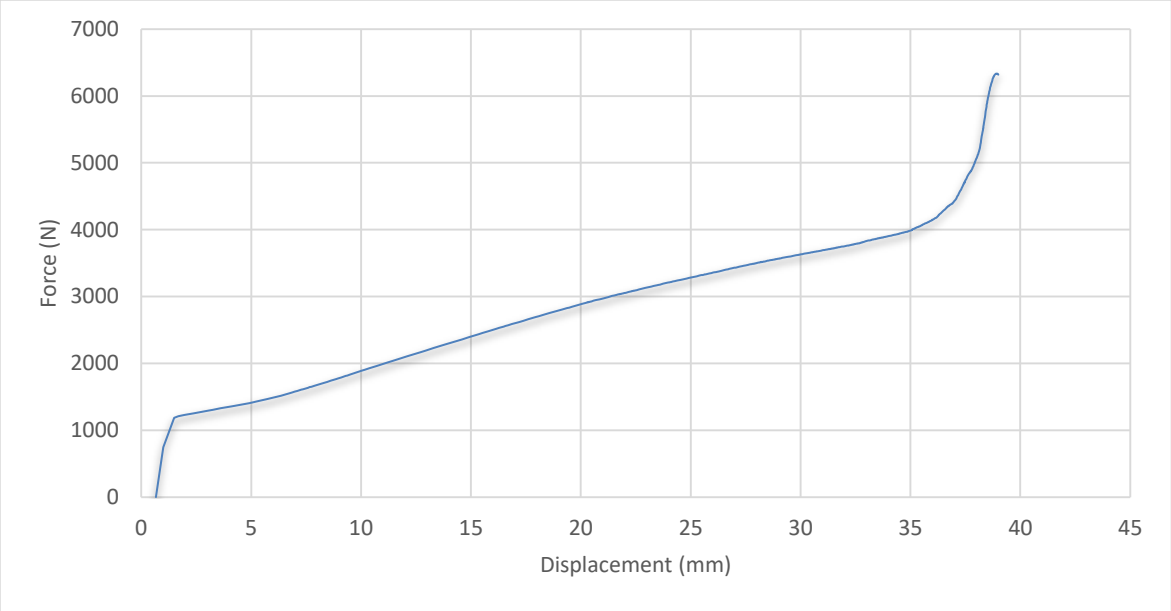

Figure 51. Reaction force on male die from paperboard against displacement.

3.2.2 Line creases pattern

The convertibility of paperboard can be enhanced by crease patterns (see Figure 53) and (see Figure 55). Creases reduce the bending stiffness and allow material to adopt complex shape.

3.2.2.1 Total strain

In simulation, creases were modelled using hinge joint which allow rotation along hinge axis. Creases reduced the effect of maximum value of total strain compared to plane paperboard (see Figure 52).

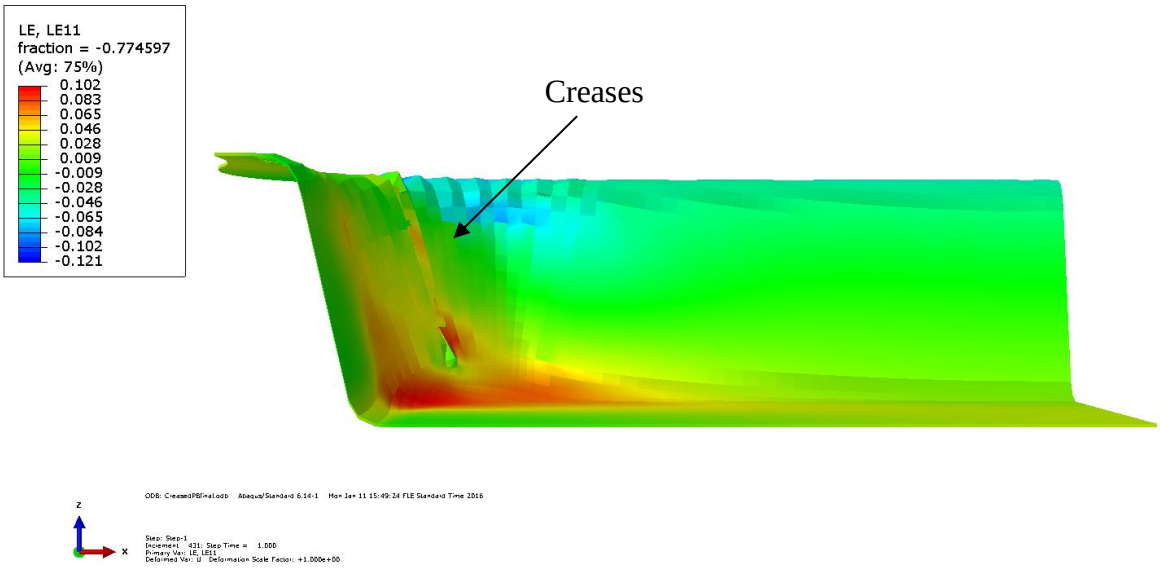

Figure 52. L11 total strain in creased single ply paperboard.

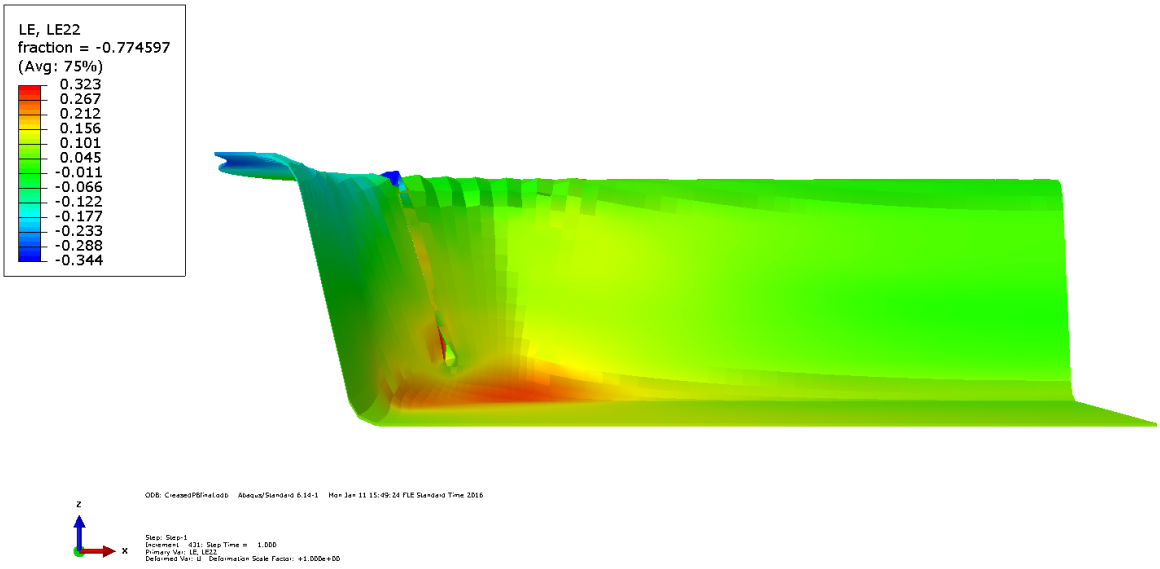

Figure 53. L22 total strain in creased single ply paperboard.

The L11 in multiply creased paperboard was higher compared to single ply paperboard because of an unexpected fold during forming. It increase the overall total strain in MD (see Figure 54).

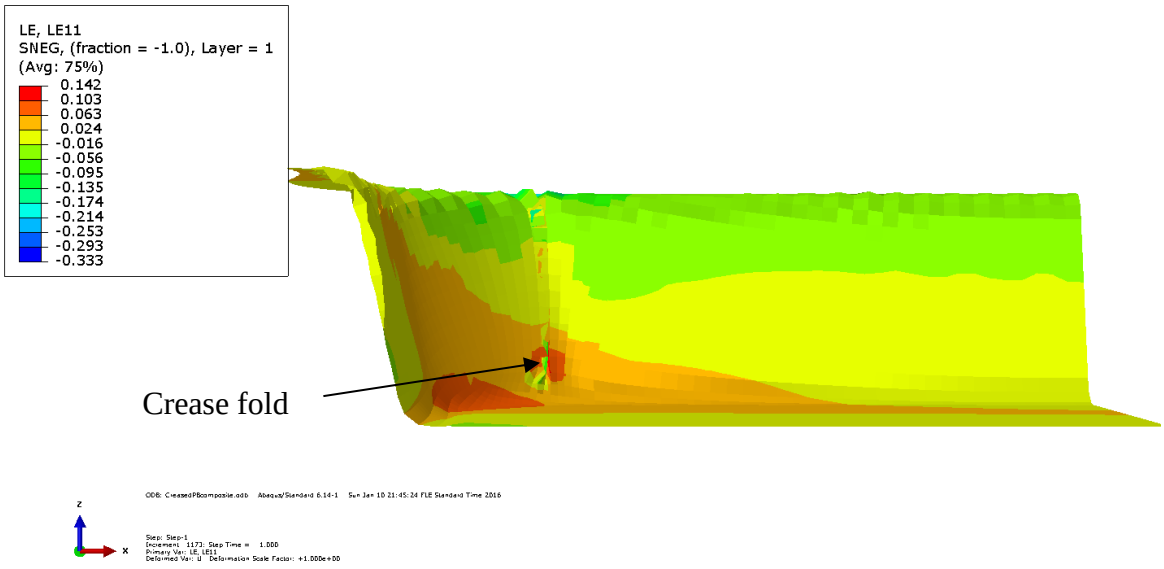

Figure 54. L11 total strain in creased multiply paperboard.

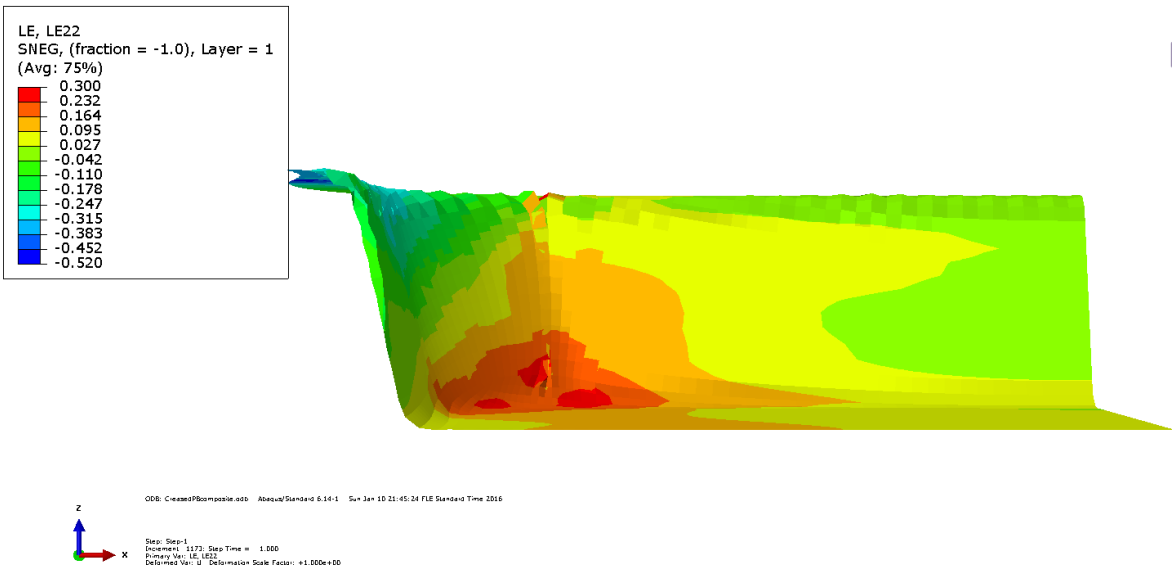

Figure 55. L22 total strain in creased multiply paperboard.

3.2.2.2 Plastic strain

The plastic strain in MD and CD with single (see Figure 56) and multiply creased paperboard (see Figure 58) is presented and compared.

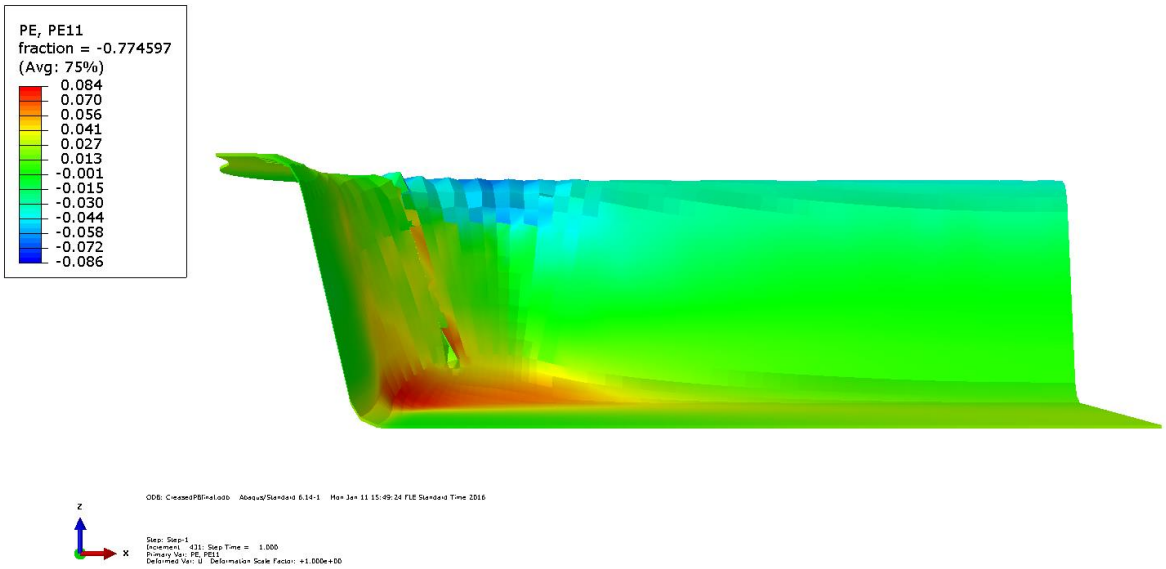

Figure 56. PE11 (MD) plastic strain in creased single ply paperboard.

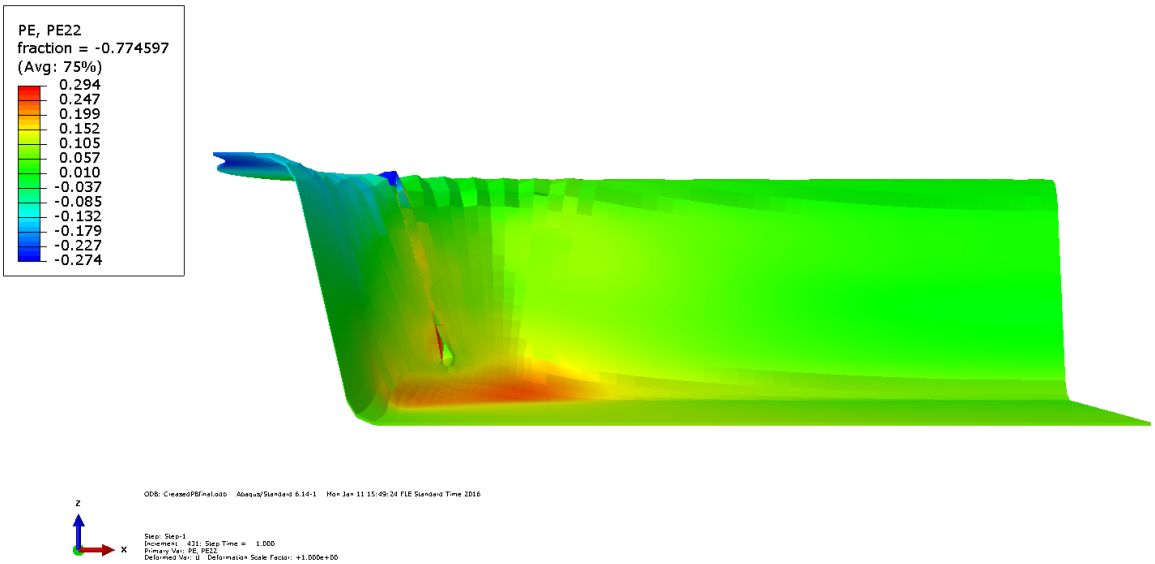

Figure 57. PE22 (CD) plastic strain in creased single ply paperboard.

The maximum plastic strain around lower corner is in between 0.19 to 0.29 because of folds in crease lines (see Figure 57).

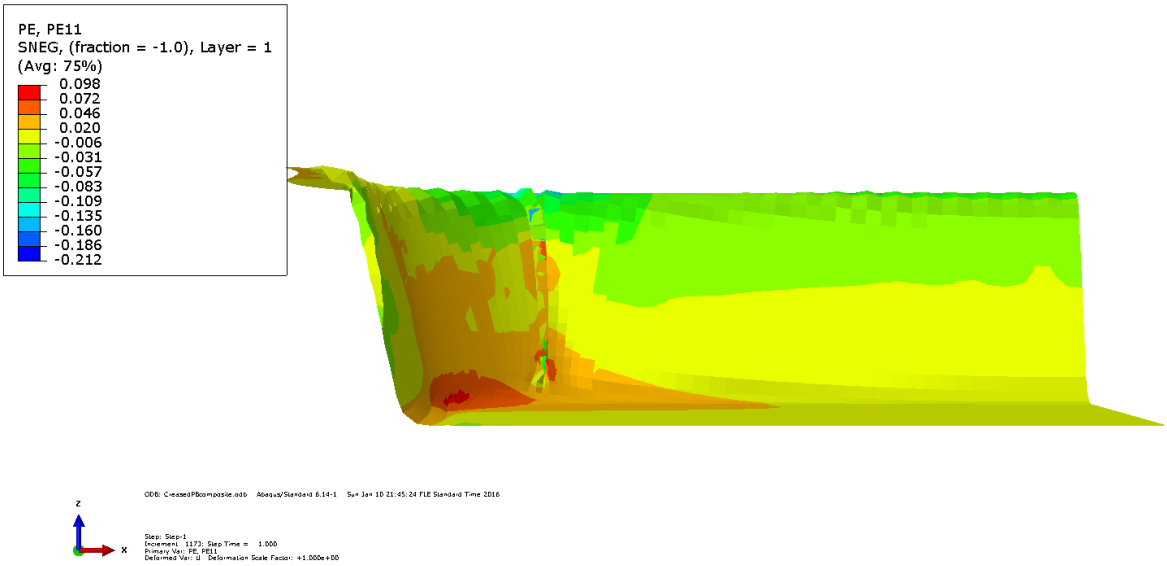

Figure 58. PE11 (MD) plastic strain in creased multiply paperboard.

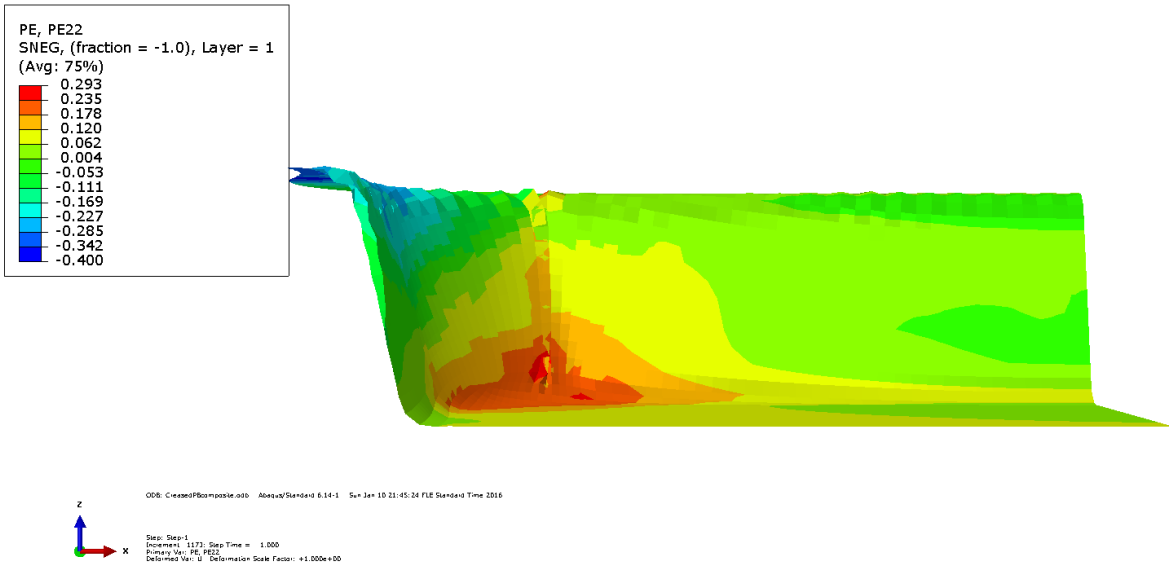

Figure 59. PE22 (CD) plastic strain in creased multiply paperboard.

The maximum plastic strain in CD around lower corner is in between 0.23 to 0.29 because of higher stress concentration (see Figure 59).

3.2.2.3 Stresses

The MD stress distribution also demonstrate the difference in stress components of both plane (see Figure 60) and creased paperboard (see Figure 62).

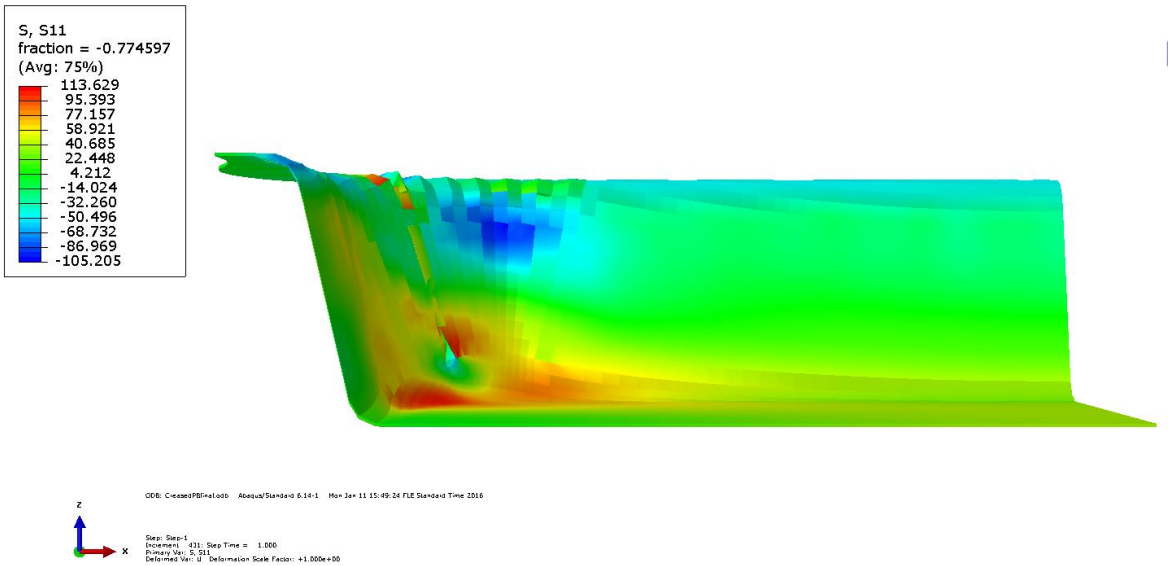

Figure 60. S11 (MD) stress in creased single ply paperboard.

The CD stress components of both plane (see Figure 61) and creased paperboard (see Figure 63) show a difference of 76.299 MPa (across red region).

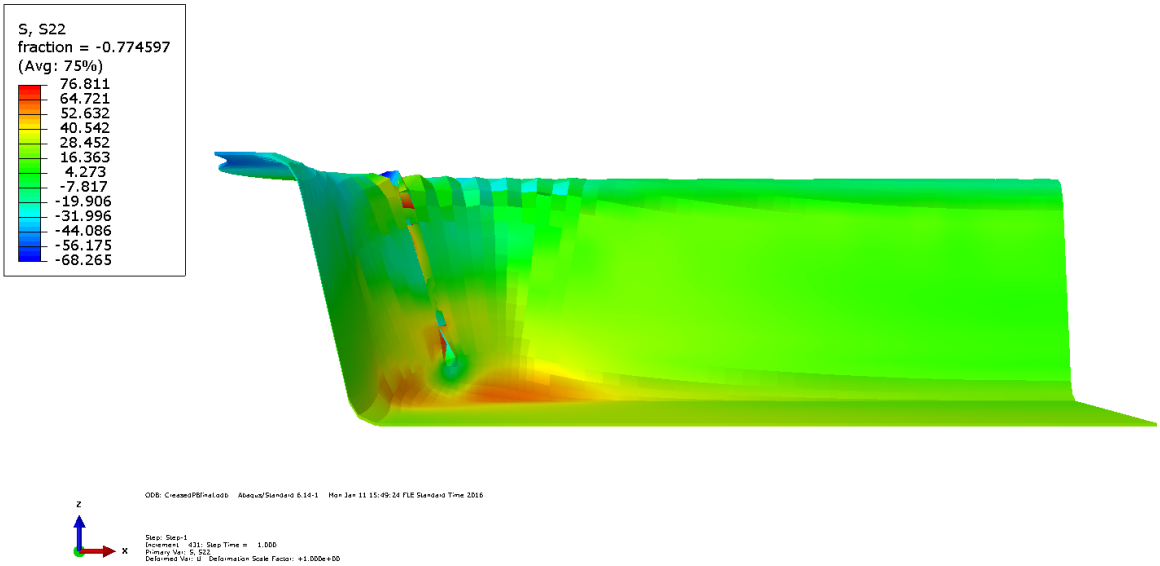

Figure 61. S22 (CD) stress in creased single ply paperboard.

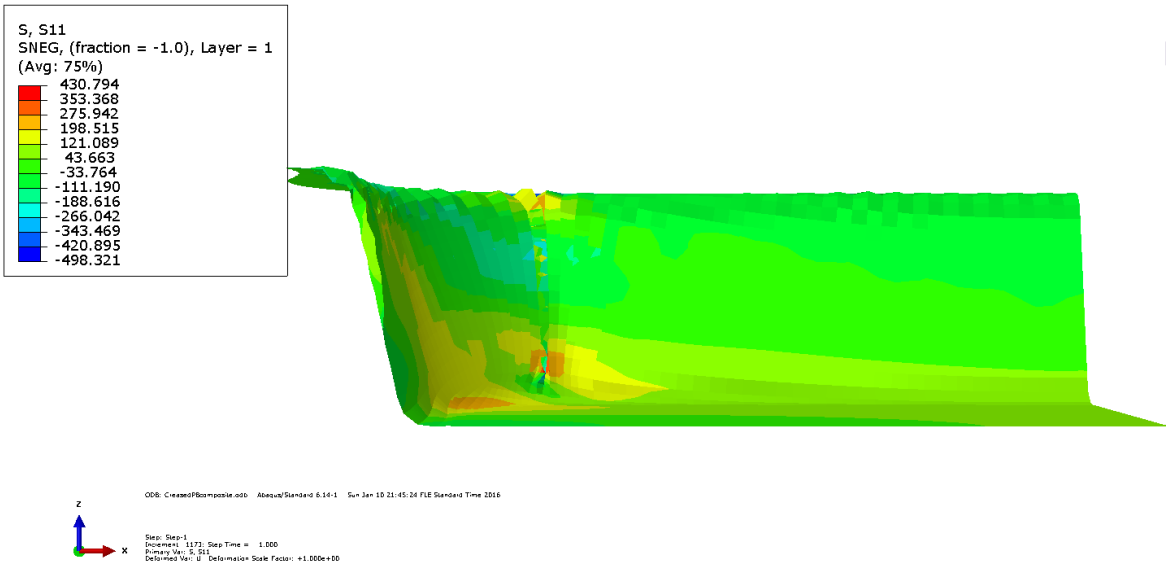

Figure 62. S11 (MD) stress in creased multiply paperboard.

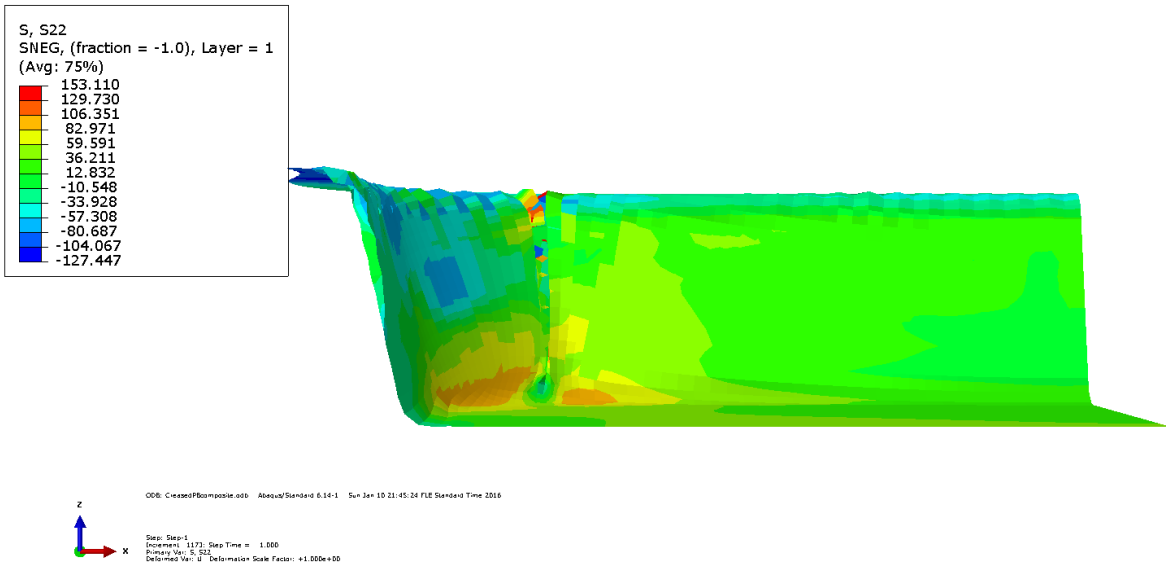

Figure 63. S22 (CD) stress in creased multiply paperboard.

3.2.2.4 Reaction force

Reactional force on male die from creased paperboard illustrated the similar behavior as plane paperboard. At the end of curve it shows a hump that expresses the required force for folding and assisting creases. Force increases until blank attain the female die geometry (see Figure 64).

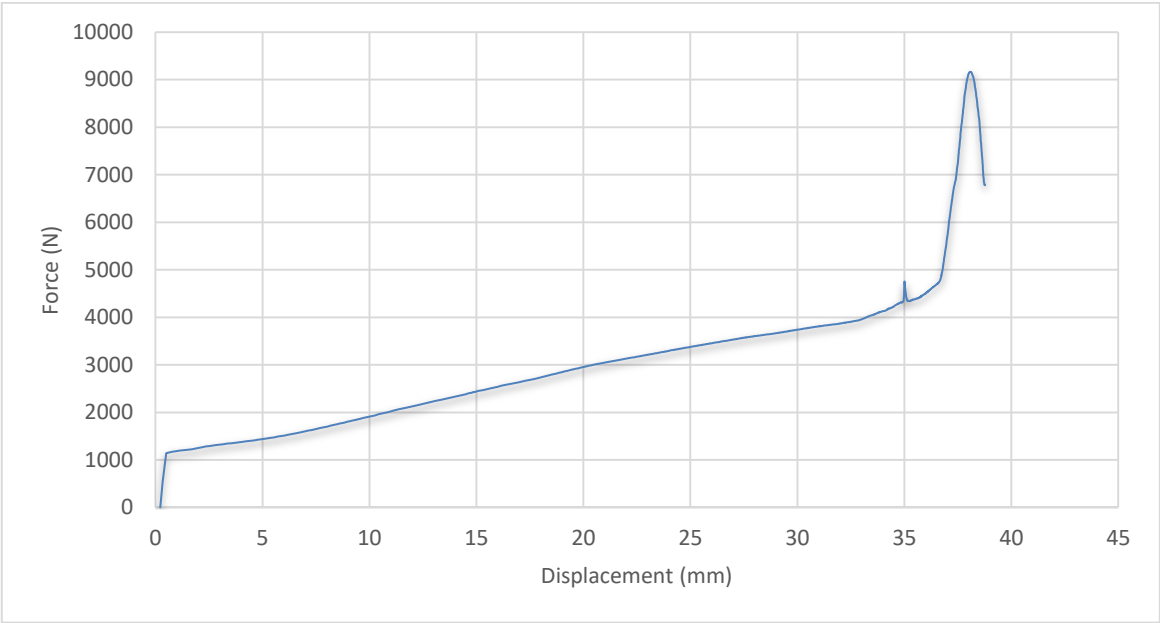

Figure 64. Reaction force on male die from creased paperboard against displacement.

3.3 Defects during forming

Shape and dimension stability of formed paperboard depends on different parameters such as material properties and fibers orientation. In simulation, material properties (orientation), boundary condition, blank holding forces and contact among surfaces causes the wrinkling and smear defects (see Figure 65).

Blank holding force during forming process plays an important role. The control of frictional force between paperboard and blank is a dominant factor for accurate geometry (see Figure 66). In actual forming process, blank holder provide releasing force to blank. If this force is lower it cause smears around round edges and elongation of upper folding of paperboard.

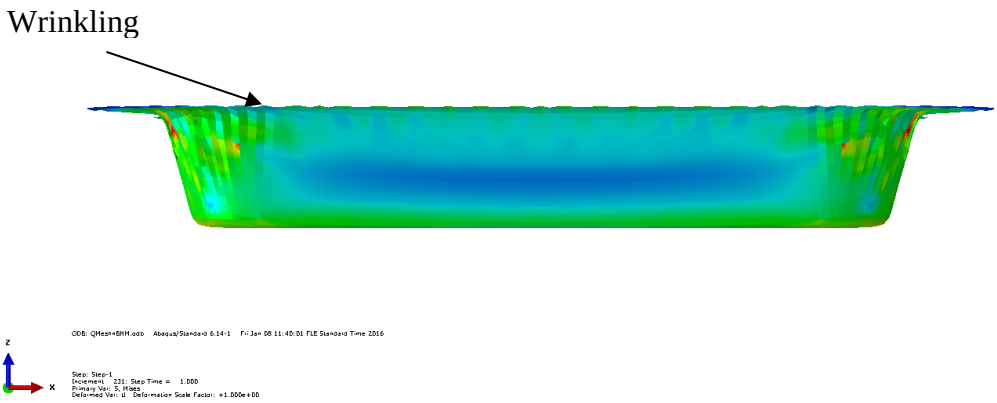

Figure 65. Wrinkling defect during paperboard forming.

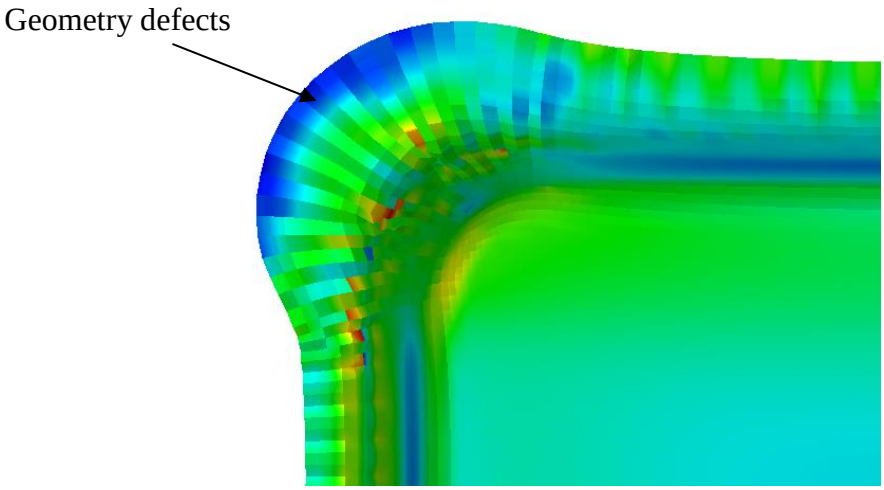

Figure 66. Geometrical defect during forming process.

4 CONCLUSION

The first objective of research was to analyze the 3D forming of paperboard by mathematical modelling and simulation. Results revealed that material model, anisotropy and boundary conditions play a vital role in convertibility of paperboard tray package.

The effect of creases during forming enhance the overall performance. Creased and plane paperboards were compared on the basis of total strain, plastic strain, stress and reactional force on male die. The results showed the fact that creases made the material less stiff and easy to deform. Slanted walls of female die were considered the position to differentiate the convertibility of plane paperboard and creased one.

The results demonstrate that total strain along MD and CD in creased paperboard was lower compared to plane paperboard. Creases enhance the convertibility of paperboard during forming process.

Reaction force curve attained from simulation results follow the similar behavior as measured in the referred study with the help of four sensors. The graph showed the stable behavior between 15 to 37 mm of displacement. The hump on curve was because of folding and crease assistance during forming.

The mathematical modelling of 3D forming process was a challenging task. The difficulties that were faced during modelling was excessive deformation, stabilization control, multiple interactions at one time, friction and interaction with creases (hinge joints). These obstacles not only restricted the modelling process, it also increased the simulation time.

5 FUTURE WORK

Many possible creasing patterns can be simulated using Abaqus. The complexity of pattern restrict the possible outcomes such as hinge joints in pentagonal and squared manner. It increase the simulation time and possibility of errors in results.

5.1 Rectangular crease pattern

Rectangular crease pattern was designed (see Figure 67). It is predicted that cross crease lines improve the elongation on 11 and 22 direction.

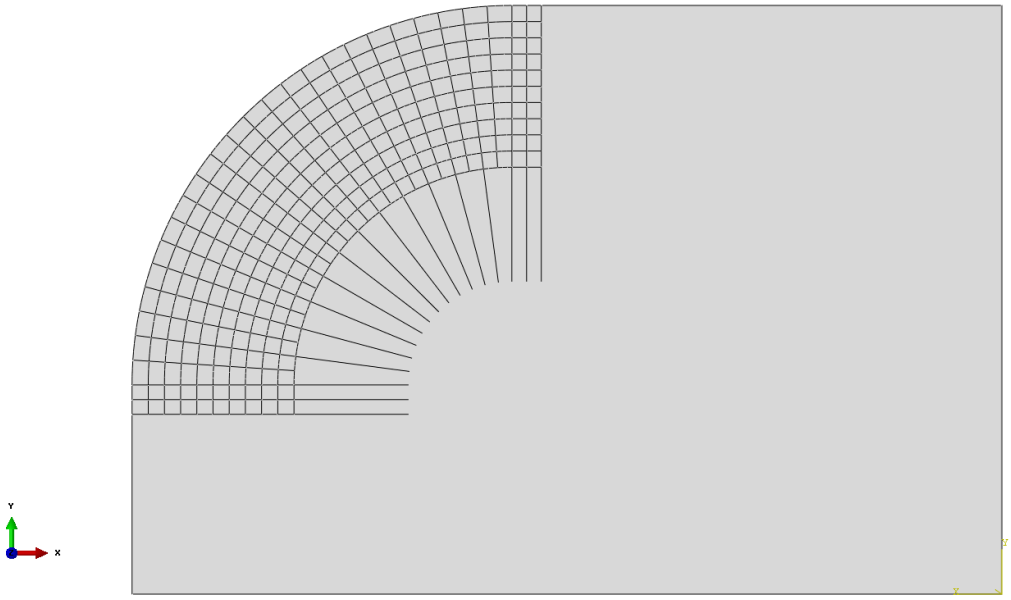

Figure 67. Rectangular creasing patterns.

5.2 Football patch pattern (Honey comb structure)

Football patch pattern was made by careful consideration of the hexagonal and pentagonal symmetry (see Figure 68). Football patch pattern was a challenging task because of limitations in Abaqus and experimental restriction.

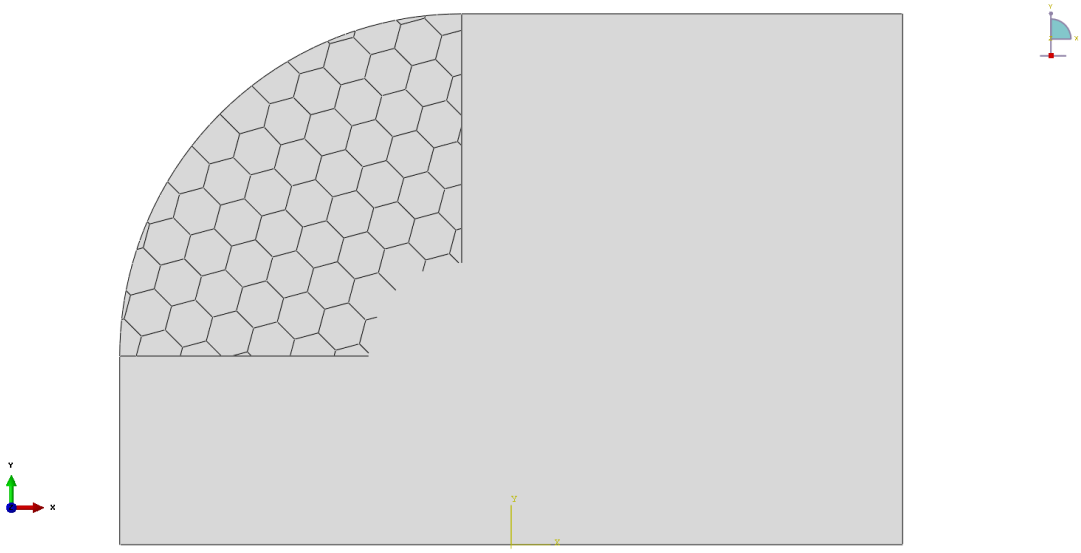

Figure 68. Honey comb structure.

LIST OF REFERENCES

Amigo, J. C. 2012. Stiffness Design of Paperboard Packages using the Finite Element Method. Master of Science Thesis. KTH School of Engineering Sciences, Department of Solid Mechanics. 66 p.

Cook, R. 1995. Finite Element Modeling for Stress Analysis. United States: John Wiley & Sons, Inc.. 320 p.

Findley, W., Lai, J., & Onaran, K. 1976. Creep and relaxation of nonlinear viscoelastic materials with an introduction to linear viscoelasticity. The Netherlands: North-Holland Pub, Co.. 389 p.

Huang, H. & Nygårds, M. 2012, Numerical Investigation of Paperboard Forming. In: Nordic Pulp and Paper Research Journal, 27: 2. Pp. 211-225.

Huang, H. 2011. Numerical and Experimental Investigation of Paperboard Creasing and Folding. Licentiate Thesis. Royal Institute of Technology, Department of Solid Mechanics. 28 p.

Huang, H. 2013. Numerical and Experimental Investigation on Paperboard Converting Processes. Doctoral Thesis. Royal Institute of Technology, Department of Solid Mechanics. 29 p.

Iggesund. 2016a, Deep drawing or thermo forming [web document]. Published 2015, updated 7.9.2015 [Referred: 15.9.2016]. Available: https://www.iggesund.com/en/knowledge/the-reference-manual/printing-and-converting-performance/deep-drawing-or-thermo-forming/

Iggesund. 2016b, Law of nature [web document]. Published 2015, updated 7.9.2015 [Referred: 15.9.2016]. Available: https://www.iggesund.com/en/knowledge/the-reference-manual/baseboard-physical-properties/laws-of-nature/

Leppänen, T., Sorvari, J., Erkkilä, A. & Hämäläinen, J. 2005, Mathematical modelling of moisture induced out-of-plane deformation of a paper sheet. In: Modelling and Simulation in Materials Science and Engineering, 13: 6. Pp. 841-850.

Stenberg, N. & Fellers, C. 2002, Out-of-plane Poisson's ratios of paper and paperboard. In: Nordic Pulp & Paper research journal, 17: 4, Pp. 387-394.

Tanninen, P. 2015. Press forming of paperboard-Advancement of converting tools and process control. Doctor of Science Thesis. Lappeenranta University of Technology, Department of Mechanical Engineering. 77 p.

Vishtal, A., Hauptmann, M., Zelm, R., Majschak, J. & Retulainen, E. 2013, 3D Forming of Paperboard: The Influence of Paperboard Properties on Formability. In: Packaging Technology and Science, 27: 9, Pp. 677–691.

Wallmeier, M., Linvillb, E., Hauptmanna, M., Majschaka, J. & Östlundb, S. 2015, Explicit FEM analysis of the deep drawing of paperboard. In: Mechanics of Materials, 89, Pp. 202–215.

Modelling Steps.

The model is described hierarchically in this Appendix I. The male die, female die and blank holder model design is describe in following steps.

$$Module \rightarrow Part \rightarrow Create\ part$$

As forming tools are made by discrete rigid, it does not allow the material to deform. Surfaces are sketched and extruded into solid rigid part and later features at different angles are introduced (see Figure 1). Later solid discrete material is transformed into shell by simply following option from main bar.

$$Shape \rightarrow Shell \rightarrow From\ Solid$$

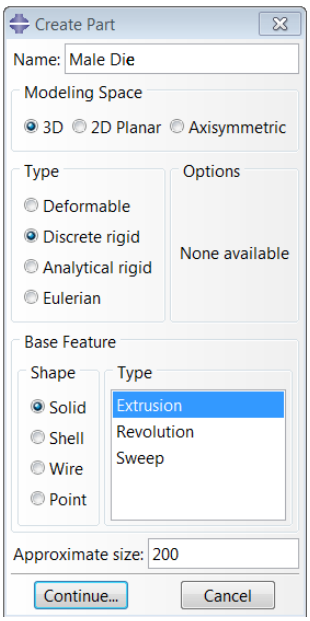

Figure 1. Creation of parts.

While on the other hand, paperboard was made by using deformable material. Base feature included shell-planar (see Figure 2).

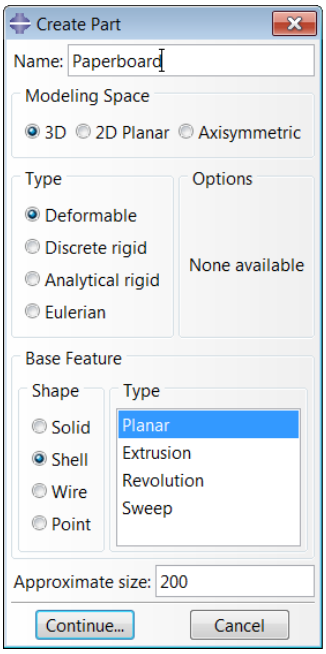

Figure 2. Creation of planar paperboard

The material was assigned by material properties that include elastic and plastic properties. In the same step, material orientation was established that show fibers orientation.

$$Module \rightarrow property \rightarrow create\ material$$

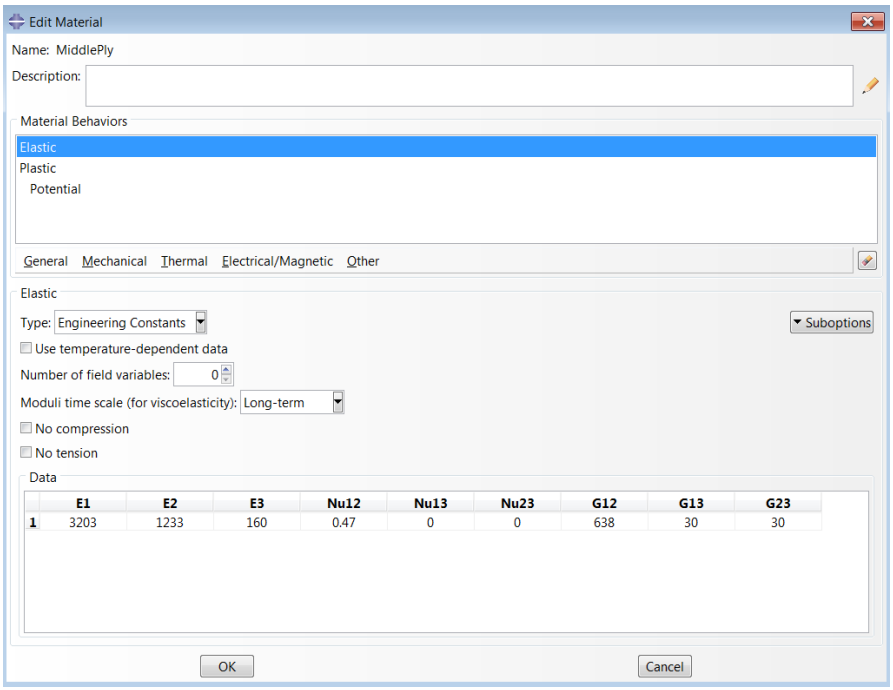

Figure 3. Creation of material (Elastic material).

Material definition was not possible to discrete material. For paperboard, first section was managed and then it was assigned to relevant geometry.

$$Module \rightarrow part \rightarrow create\ \text{section}$$

Paperboard was treated as homogenous material with geometric feature of shell. Properties across the whole dimensions acted as homogeneous distribution.

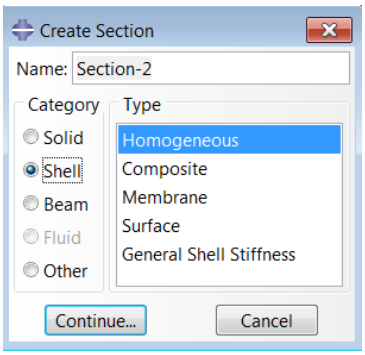

Figure 4. Homogeneous structure of paperboard.

Paperboard was then assigned material properties. In section assignment, layer of paperboard was selected from which it differentiate the top and middle layers.

$$Module \rightarrow part \rightarrow Section\ assign$$

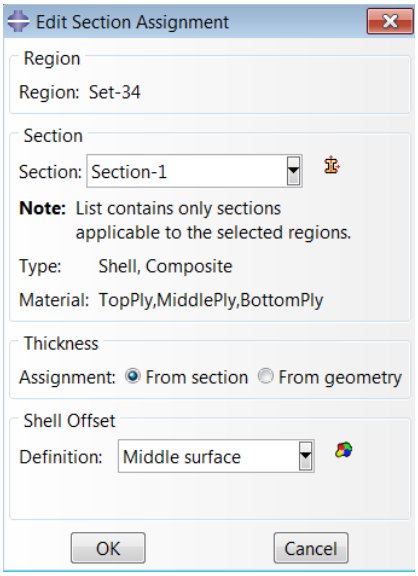

Figure 5. Material assignment for paperboard.

After the creation of part, assembly with consideration of tolerance and mechanism was made. Each instance was separated at specific distance.

$$Module \rightarrow assembly \rightarrow Create\ Instance$$

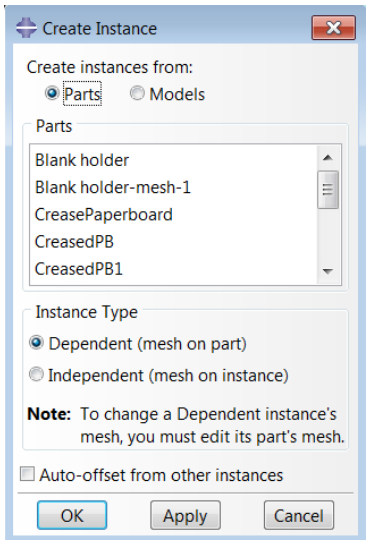

Figure 6. Creation of assembly.

$$Module \rightarrow assembly \rightarrow Rotate\,Instance$$

$$Module \rightarrow assembly \rightarrow Translate\,Instance$$

Forming process include interaction between parts. The contact between male die and female die was generated by surface to surface contact tool in interaction module. Similarly contact between female die, blank holder and blank was created. In Abaqus, calculation regarding to contact sometime cause problem in convergence.

$$Module \rightarrow Interaction \rightarrow Create\ interaction$$

Master and slave surface was distinguished. Paperboard surface was treated as slave surface while rest of the discrete parts were dealt as master surface. A slave properties cannot be assigned to discrete rigid parts.

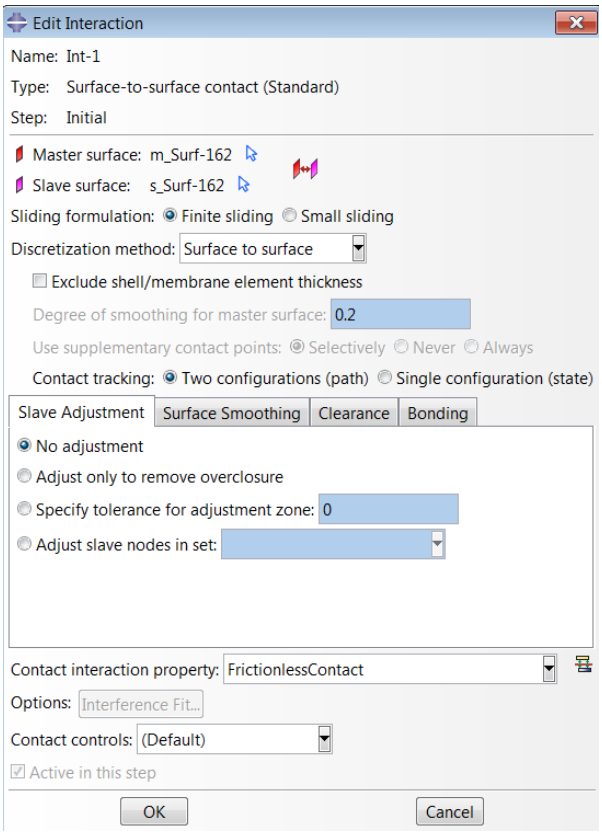

Figure 7. Interaction definition between master and slave surfaces.

In contact properties friction between male die and paperboard was defined that was 0.20, whereas friction coefficient between female die and blank was very less 0.01.

Module→Interaction→Create interaction properties

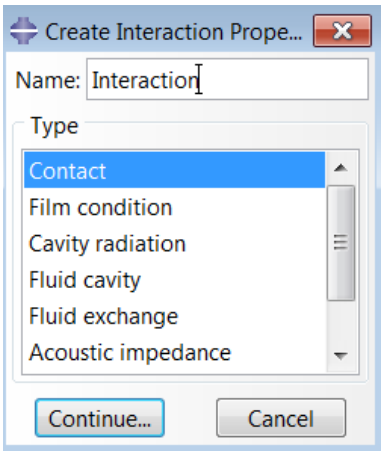

Figure 8. Creation of interaction properties.

Creation of hinge joint in order to interpret creases can be made by interaction module. In current research, it was made by Python codes that dealt with connector element and assignment.

Module→*Interaction*→ *Create connector section*

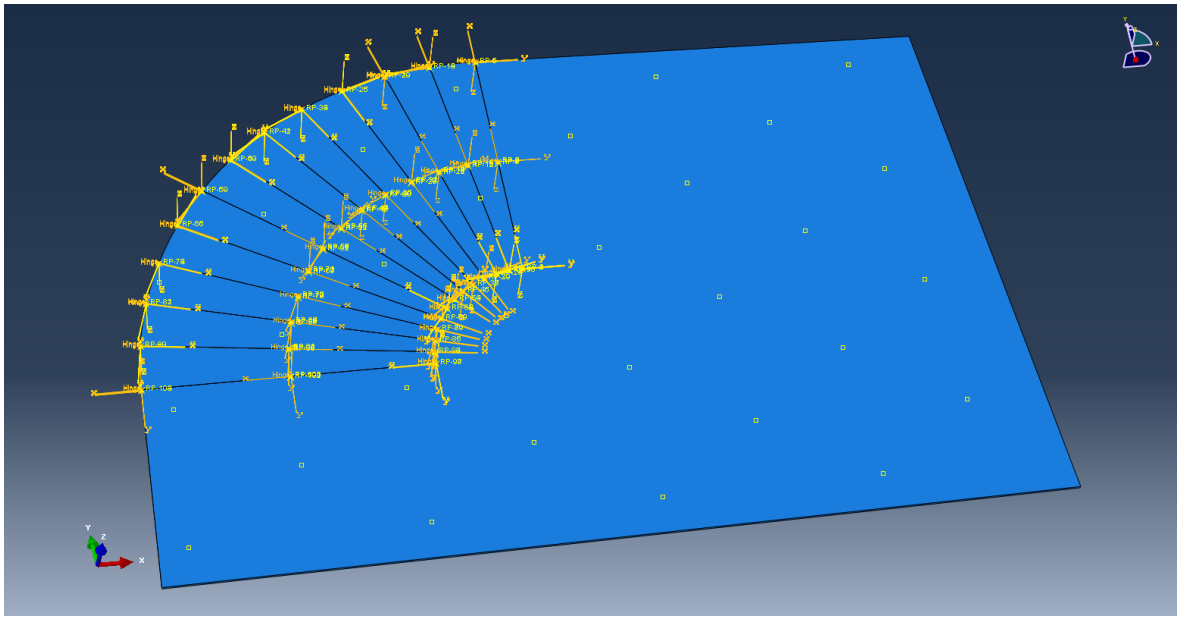

Figure 9. Connector (hinge joint) to interpret creases on paperboard.

In order to mesh the individual parts, global size of each part was chosen. All types were assigned S3 mesh element type.

$$Module \rightarrow Mesh \rightarrow Mesh\ part$$

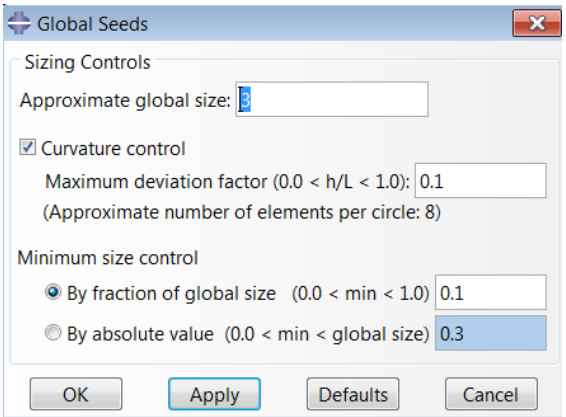

Figure 10. Global seeding of mesh parts.

Finally, for forming of paperboard 'Static, general' analysis was selected and the parameter NLGEOM was activated (see Figure 11).

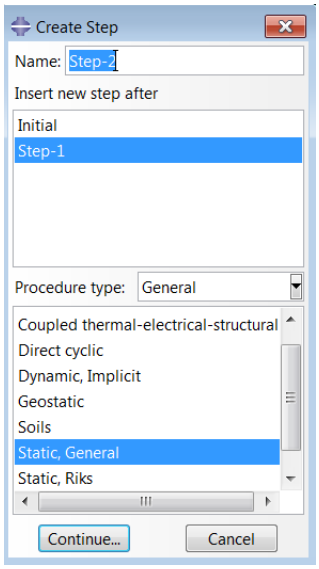

Figure 11. Creation of static analysis.

Furthermore, because of excessive deformation, specific damping factor was activated (see Figure 12).

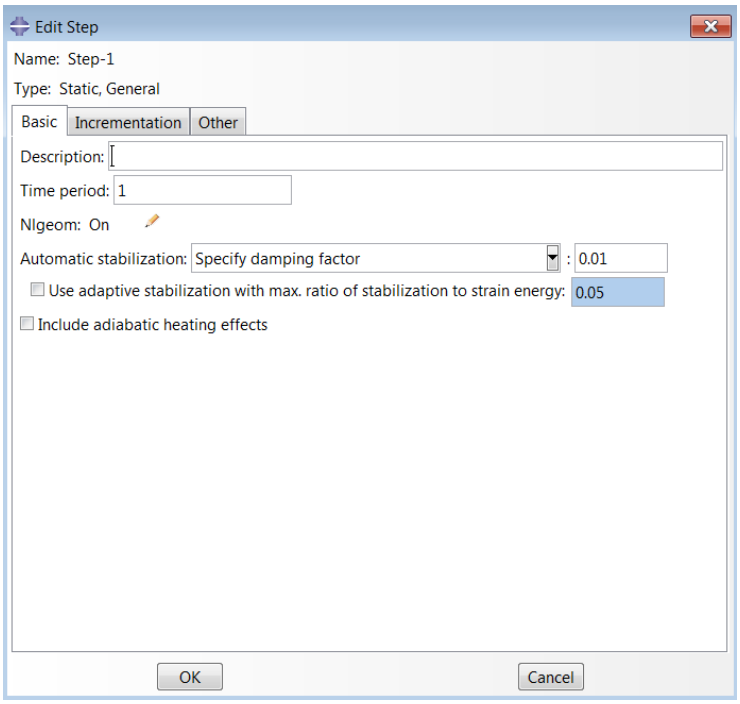

Figure 12. Setting of NLGEOM on.